Anti-GD1a antibodies activate complement and calpain to injure distal motor nodes of Ranvier in mice

McGonigal R[1], Rowan EG[2], Greenshields KN[1], Halstead SK[1], Humphreys PD[1], Rother RP[3], Furukawa K[4], Willison HJ[1]

[1]Division of Clinical Neurosciences, Glasgow Biomedical Research Centre, University of Glasgow, Glasgow G12 8TA

[2]Strathclyde Institute of Pharmacy and Biomedical Sciences, Sir John Arbuthnott Building, University of Strathclyde, Glasgow G4 0NR

[3]Alexion Pharmaceuticals, Cheshire, CT 06410, USA

[4]Department of Biochemistry II, Nagoya University Graduate School of Medicine, Nagoya, Japan

Address for correspondence:

Professor Hugh J. Willison,

University of Glasgow Division of Clinical Neurosciences,

Glasgow Biomedical Research Centre, Room B330

120 University Place, Glasgow, G12 8TA, Scotland.

Tel: 44 (0) 141 330 8384

e-mail: h.j.willison@clinmed.gla.ac.uk

Running head: Anti-GD1a antibody-mediated nodal injury (40 characters)

Word count: (excludes refs and legends) 7633

Abstract

The motor axonal variant of Guillain-Barré syndrome is associated with anti-GD1a IgG antibodies which are believed to be the pathogenic factor. In previous studies we have demonstrated the motor terminal to be a vulnerable site. Here we show both *in vivo* and *ex vivo* that nodes of Ranvier in intramuscular motor nerve bundles are also targeted by anti-GD1a antibody in a gradient-dependent manner, with greatest vulnerability at distal nodes. Complement deposition is associated with prominent nodal injury as monitored with electrophysiological recordings and fluorescence microscopy. Complete loss of nodal protein staining, including voltage-gated sodium channels and ankyrin G, occurs and is completely protected by both complement and calpain inhibition, although the latter provides no protection against electrophysiological dysfunction. In *ex vivo* motor and sensory nerve trunk preparations, antibody deposits are only observed in experimentally desheathed nerves, which are thereby rendered susceptible to complement-dependent morphological disruption, nodal protein loss and reduced electrical activity of the axon. These studies provide a detailed mechanism by which loss of axonal conduction can occur in a distal dominant pattern as observed in a proportion of motor axonal Guillain-Barré syndrome patients, and also provide an explanation for the occurrence of rapid recovery from complete paralysis and electrophysiological in-excitability. The studies also identify therapeutic approaches in which nodal architecture can be preserved.

Abbreviations: α-BTx, α-bungarotoxin; AMAN, acute motor axonal neuropathy; BNB, blood nerve barrier; CAP, compound action potential; CFP, cyan fluorescent protein, CFP; GBS, Guillain-Barré syndrome; GD3s, GD3 synthase; LOS, lipo-oligosaccharides; LTx, alpha-latrotoxin; mAb, monoclonal antibody; MAC, membrane attack complex; NF, neurofilament; NHS, normal human serum, NoR; node of Ranvier; PBS, phosphate-buffered saline; TTx, tetrodotoxin; TS, triangularis sternae; RT, room temperature; WT, wild type.

Introduction

The motor axonal variant of Guillain-Barré syndrome (GBS), termed acute motor axonal neuropathy (AMAN) (Feasby *et al.,* 1986;Hughes and Cornblath 2005;McKhann *et al.,* 1993) characteristically follows *Campylobacter jejuni* infection and is associated with serum anti-GM1, -GD1a and -GalNAc-GD1a ganglioside antibodies (Ho *et al.,* 1999;Lugaresi *et al.,* 1997;Ogawara *et al.,* 2000). AMAN-associated *Campylobacter jejuni* strains have ganglioside-like surface lipo-oligosaccharides (LOS) Aspinall *et al.,* 1993) suggesting induction is due to a mechanism of molecular mimicry, which has been proven experimentally (Ang *et al.,* 2004;Goodyear *et al.,* 1999).

Gangliosides are sialic acid-containing glycosphingolipids expressed at high levels in the nervous system in a range of cell-specific patterns (Ledeen 1978). Gangliosides have diverse functions related to neural development, maintenance and regeneration, including stabilising the axo-glial junction at the node of Ranvier (NoR) (Sheikh *et al.,* 1999b;Susuki *et al.,* 2007a;Silajdzic *et al.,* 2009). Although no specific neural function has been attributed to GD1a, it has been identified in the motor nerve terminal and nodal axolemma (De Angelis *et al.,* 2001;Gong *et al.,* 2002;Goodfellow *et al.,* 2005;Sheikh *et al.,* 1999a), sites which correspond to those predicted from clinical, electrophysiological and pathological data to be affected in motor axonal forms of GBS (Griffin *et al.,* 1996;Ho *et al.,* 1997;Kuwabara *et al.,* 2004).

The distal motor nerve, nerve terminal and ventral roots have relatively higher permeability to circulating factors than nerve trunks, owing to local variations in the protective properties of the blood nerve barrier (BNB) (Burkel 1967;Malmgren and Olsson 1980;Olsson 1990;Saito and Zacks 1969). These BNB variations could allow circulating antibody access to either very distal or very proximal motor axonal membranes and thereby account for more targeted injury to these regions. Thus it has been proposed that one explanation for the very rapid recovery from paralysis seen in some AMAN patients could be due to axonal conduction block at the distal motor axon and nerve terminal, a site with the capacity to regenerate rapidly (Goodfellow *et al.,* 2005;Ho *et al.,*1997). Conversely, severe proximal axonal injury resulting in widespread axonal degeneration that overwhelmed the compensatory capacity of motor unit remodelling would inevitably lead to permanent motor axonal deficits, as is seen in some AMAN cases (Hiraga *et al.,* 2005a;Hiraga *et al.,* 2005b).

Several anti-GM1 and -GD1a ganglioside antibody-mediated mouse and rabbit models of AMAN have been generated (Goodfellow *et al.,* 2005;Sheikh *et al.,* 2004;Susuki *et al.,* 2003). Models to date have focused on sciatic nerve and ventral root axons, or on axonal components of neuromuscular junctions. In a passive immunisation mouse model of AMAN mediated by anti-GD1a antibody supplemented with guinea pig complement, axonal injury was observed in spinal roots and sciatic nerve (Sheikh *et al.,* 2004). Similarly in a rabbit model induced by active immunisation with GM1, axonal injury was observed in spinal roots, in which rabbit complement deposits were also evident (Susuki *et al.,* 2003).

Extensions of this study focussing on the NoR revealed destabilisation of nodal and paranodal structures, including loss of sodium (NaV) channels, findings interpreted as the consequence of antibody and complement-mediated axo-glial disruption(Susuki *et al.,* 2007b), and their protection with a complement inhibitor (Phongsisay *et al.,* 2008).

These complement mediated effects at the NoR in the ventral root mirror those demonstrated in patient autopsy tissue (Hafer-Macko *et al.,* 1996). As the NoR is vital for impulse propagation (Poliak and Peles 2003;Scherer 1996), understanding AMAN immunopathology at this site in relation to function is both critical and complex. The NoR is organised into 3 subdomains - the nodal gap, the paranode and the juxtaparanode (Fig. S8). The voltage-gated sodium channel isoform Nav1.6 is expressed at the NoR (Caldwell *et al.,* 2000), along with the cytoskeletal protein ankyrin G (Kordeli *et al.,* 1990) and the cell adhesion molecules neurofascin 186 and NrCAM (Davis *et al.,* 1996). At the paranode, the axo-glial junction is formed by the axolemmal proteins contactin and Caspr, while neurofascin 155 is the glial receptor to this complex (Charles *et al.,* 2002;Einheber *et al.,* 1997;Menegoz *et al.,* 1997;Peles *et al.,* 1997;Rios *et al.,* 2000;Tait *et al.,* 2000). The axo-glial junction acts as a barrier to prevent lateral movement of nodal constituents, thus organising the channel clustering required for maintenance of membrane potentials (Bhat *et al.,* 2001;Boyle *et al.,* 2001). At the juxtaparanode, voltage-gated potassium channels localised on the axon, in complex with Caspr 2 and Tag1 (Arroyo *et al.,* 1999;Wang *et al.,* 1993), play a role in repolarisation the resting membrane potential following an action potential

(Poliak and Peles2003;Rasband *et al.,* 2002;Traka *et al.,* 2002). Glycosyltransferase knockout mouse studies indicate that GD1a or related gangliosides clearly modulate the structural and functional integrity of this site, although the precise mechanisms are poorly understood (Sheikh *et al.*,1999b;Silajdzic *et al.*, 2009;Susuki *et al.*, 2007a).

In our *ex vivo* mouse model of AMAN, motor nerve terminals enriched in GD1a develop severe functional and pathological injury when exposed to anti-GD1a antibody with complement activation(Goodfellow *et al.*, 2005). The pore forming action of complement is critical to the development of this injury and that mediated by other anti-ganglioside antibodies, in part through allowing uncontrolled calcium influx into the nerve terminals, with subsequent Ca^{2+}-dependent protease, calpain, activation and cleavage of structural proteins in the axon terminal (O'Hanlon *et al.,* 2003).

This study set out to assess whether anti-GD1a-antibody mediated injury could be observed to occur at NoR in the distal portions of the axon, upstream from the motor nerve terminal. If present, we also intended to determine the mechanism of action and functional effects of any observed injury that might lead to therapeutic intervention, analogous to our previous approach to the neuromuscular junction.

Materials and methods

Mice

Male GD3 synthase knockout mice (GD3s$^{-/-}$) mice (Okada *et al.,* 2002) were crossed with B6/Cg-TgN(Thy1-CFP) x DBA mice that endogenously express cyan fluorescent protein (CFP) in their axons (Feng *et al.,* 2000, kindly provided by Dr W. Thompson, Austin, Texas) to produce a doubly genetically modified mouse referred to as GD3s$^{-/-}$/CFP in this study. GD3s$^{-/-}$ mice were preferentially used as they express greater amounts of axonal GD1a compared with their wild type (WT) counterparts, owing to blockade of b-series biosynthesis and consequent accumulation of a-series gangliosides including GD1a. The ganglioside biosynthetic pathway illustrating this is shown in Fig. S1. Through virtue of expressing high amounts of GD1a, GD3s$^{-/-}$ mice bind more anti-GD1a antibody than their wildtype (WT) counterparts as previously reported at motor nerve terminals (Goodfellow et al., 2005). In order to confirm that GD3s$^{-/-}$/CFP were an appropriate cross in which to model these experiments, binding of anti-GD1a antibody was quantified in GD3s$^{-/-}$/CFP mice in comparison with WT/CFP controls (Fig. S2). Mice were killed by CO_2 inhalation at 6-12 weeks of age and experiments were carried out under licence (PPL60/3842) in accordance with UK Home Office guidelines.

Antibodies and reagents

The IgG2b mAb to GD1a (herein termed anti-GD1a antibody, also known as MOG-35) was produced by immunisation of GalNAcT$^{-/-}$ mice (lacking all complex gangliosides (Takamiya *et al.,* 1996), with the *Campylobacter jejuni* HS:19 LOS strain that possesses structures identical to GD1a to which it raises a cross-reactive immune response (Bowes *et al.,* 2002)] and acts as an antecedent infection in AMAN, as described (Boffey *et al.,* 2005). Antibodies to channels, other proteins and membrane attack complex (MAC), C5b-9 are detailed in Table 1. Eculizumab, a humanised anti-human C5 mAb that binds plasma C5 to prevent MAC formation and ALXN3300 (the isotype-matched control mAb) were supplied by Alexion Pharmaceuticals (Cheshire, USA). The synthetic peptide AK295 binds calpain I, II and cathepsin B to prevent their activation and proteolytic action (Li *et al.,* 1996). Toxins were used as follows: α-bungarotoxin (BTx, Molecular Probes, UK) Alexa Fluor 488 and 647 conjugates at 1:500; α-latrotoxin (LTx, Alomone Labs, Israel) at 12nM; tetrodotoxin (TTX, Biotium Inc, USA) at 5μM; vecuronium (Organon Laboratories Ltd, Cambridge, UK) at 5μM.

Ex vivo and in vivo muscle and nerve permeability studies
Triangularis sterni (TS) muscle, phrenic nerve, sural nerve and sciatic nerve were dissected, mounted and maintained alive in Ringer's medium (116mM NaCl, 4.5mM KCl, 1mM $MgCl_2$, 2mM $CaCl_2$, 1mM NaH_2PO_4, 23mM $NaHCO_3$, 11mM glucose, pH 7.4) pre-gassed with 95% O_2/5% CO_2 at room temperature (~20°C). Muscle and nerve (desheathed by slitting and opening the epineurium with a fine needle, or left intact) were incubated with 100μg/ml anti-GD1a antibody for 2h at

32°C, 30mins at 4°C and a final 10mins at RT, plus BTx to label NMJ. Antibody control preparations were incubated with Ringer's alone. Preparations were rinsed in Ringer's prior to fixation in 4% paraformaldehyde (20mins, RT). Tissue was then rinsed in PBS, 0.1M glycine and PBS (10mins each, R.T.). Tissue was incubated with anti-IgG2b-FITC (1:200) and the pan anti-neurofascin antibody NFC2 (1:1000) with 0.5% Triton X-100 in blocking solution (1% goat serum and 1% L-lysine) overnight at 4°C. Intramuscular nerve bundles were divided into four categories for quantification: single fibres, small bundles (<15µm), medium bundles (15-35µm) and large bundles (>35µm). NoR were identified by neurofascin staining and the anti-GD1a antibody immunofluorescence at this region were measured within each category and compared to control tissue. To study the binding of antibody *in vivo*, the same quantification was performed on TS muscle removed from a mouse injected i.p. 16h previously with 3mg anti-GD1a antibody. PBS was used for control groups.

For sciatic, sural and phrenic nerves, in order to assess antibody and complement access through the relatively impermeable epineurium, and therefore vulnerability to injury, isolated nerves were incubated *ex vivo* with anti-GD1a antibody under intact and desheathed conditions. It was thereby established that desheathing was essential for achieving anti-GD1a antibody binding at NoR in nerve trunks, and that under these conditions antibody binding levels were equivalent to intramuscular nerve NoR. Data for the phrenic nerve is shown in Fig. S3. All studies on nerve trunks were thus conducted on desheathed nerves.

Ex vivo preparations for complement activation and nodal protein disruption

Muscle and nerve preparations were subjected to the same protocols as used for assessing permeability, with the additional step that tissue was incubated with 40% normal human serum (NHS) for 3h at RT prior to fixation. Muscle was cryosectioned at 10µm and stained for MAC, nodal channels and other proteins overnight at 4°C as listed in Table 1. In order to identify NoR, fluoromyelin green (1:400) that labels lipids, or dystrophin (1:200) that labels the myelin sheath were applied. Secondary antibodies were applied for 3 hrs at RT as follows: anti-rabbit IgG-Cy5 (1:300) for Nav1.6, Caspr, NFC2, Kv1.1, neurofilament; anti-mouse IgG1-Cy5 (1:300) for ankyrin G, moesin, NrCAM and dystrophin; anti-mouse IgG2a-TRITC (1:200) for MAC. NoR with a normal immunostaining pattern for nodal proteins were scored as present or absent/abnormal. To determine whether any abnormal immunostaining was dependent on nodal MAC deposition, or resultant from an upstream effect of massive synaptic injury, Nav1.6 immunostaining at NoR was compared between antibody treated and α-LTx treated tissue. Our previous studies have shown that the nerve terminal effects of antiganglioside antibodies mimic those of α-LTx (Plomp *et al.,* 1999;Plomp and Willison 2009) . α-LTx was added at 2nM in Ringer's to the organ bath at the same time NHS was added in a parallel preparation.

To assess the contribution of MAC to any observed injury, the C5 inhibitor Eculizumab was added at 100µg/ml to NHS 10mins prior to incubation with the muscle. To investigate the contribution of calpain, 100µM of the calpain inhibitor

AK295 (kindly provided by Dr J. Powers and J. Glass, Atlanta, Georgia), was added concurrently with NHS. Eculizumab concentration had been previously optimised (Halstead *et al.,* 2008b). AK295 was optimised for concentration by dose ranging studies from 25-200 micromolar concentrations and the lowest concentration that fully protected protein cleavage was used. In Eculizumab-treated and -unprotected intramuscular axons, the presence of axonal CFP was used to monitor axonal integrity. After AK295 treatment, the intensity of neurofilament immunoreactivity was quantified at the nerve terminal as delineated by BTx staining and compared to AK295-unprotected tissue levels. The efficacies of Eculizumab and AK295, as monitored by immunostaining profiles, were expressed as the percentage of protected versus unprotected signals at the relevant NoR sites.

Perineural and extracellular recordings

TS nerve-muscle preparations were freshly dissected and set up *ex vivo* for electrophysiological recordings as for immunocytochemisrty studies. Experiments were carried out at room temperature (20-22°C) using 2 M NaCl-filled microlectrodes with a resistance of 25-45 MΩ in preparations bathed in Ringer's. Recordings were made from nerve terminals and small and large intramuscular nerve bundles after anti-GD1a antibody incubation followed by NHS for 3hrs. Perineural waveforms associated with nerve terminal action potentials were made as previously described (Braga *et al.,* 1991). Muscles were paralysed with 5 µM vecuronium to prevent twitching. In some experiments the same

microelectrode was used to measure muscle resting membrane potentials. Signals were amplified, recorded and analysed as per the nerve extracellular recordings below.

For extracellular recordings, nerves were mounted in a custom made Perspex recording block across three chambers and sealed in with vacuum grease. Nerves were stimulated with a Grass S88 stimulator delivering pulses at a frequency of 1Hz, and at a supramaximal voltage. Signals were amplified via a CED1902 and digitised by a NIDAQ-MX A/D converter (National Instruments, Austin, Texas), then captured and analysed using WinWCP version 4.1.0 software. Phrenic nerves and sural nerves remained in the recording chamber throughout the experiments and recordings were made for 2h on the application of NHS. Recordings from the larger sciatic nerve were collected on transfer of the nerve to the recording chamber following NHS treatment in a petri dish, as penetration of NHS into the nerve was not uniformly maximal whilst in the recording chamber. At the termination of all experiments 5µM TTX was added to the recording chamber to confirm that the waveform being recorded was the result of the opening of sodium channels. A representative graph of the positive peak value of compound action potential (CAP) over time was plotted to convey conduction. A minimum of 200 control waveforms were averaged prior to the addition of NHS. Absolute CAP values were not presented as these varied between experiments; instead the percentage of the starting CAP peak value was calculated for each of 3-5 preparations and averaged for each treatment group. A 2-sample t-test was used for comparison of phrenic and sural nerve

conduction, whilst a paired t-test was performed for comparison of sciatic nerve CAP recordings.

Image acquisition and analysis

Fluorescent images were captured on both a Zeiss Axio Imager Z1 with ApoTome attachment and a Zeiss Pascal confocal laser scanning microscope. Image analysis was carried out using ImageJ software. For quantitative analysis of antibody and MAC deposition, the fluorescence signal at the region of the NoR was measured and any background fluorescence subtracted. Where relevant, measurements were categorised by bundle size as described above. The same procedure was carried out for the quantitation of neurofilament signal over the motor endplate. Measurements were pooled from three experimental preparations and presented as box and whisker plots to represent the spread of the non-parametric data. Mann-Whitney mean rank test was used to compare possible statistical differences between groups where the level of significance was set at 1%. For comparison of nodal protein immunostaining, NoR positive for individual markers were counted for each bundle category and the chi-squared test used at a 1% level of significance.

Results

Anti-GD1a antibodies are preferentially deposited at distal motor nerve nodes of Ranvier.

Anti-GD1a antibody was applied to TS muscle preparations from GD3s$^{-/-}$/CFP mice maintained *ex vivo* in organ baths and its deposition immunolocalised and quantified at the NoR in double staining studies. Anti-GD1a antibody binds intensely at the motor nerve terminal of GD3s$^{-/-}$ mice (Fig. 1A; upper area of image) as shown in previous studies (Goodfellow et al., 2005). In relation to the present study, anti-GD1a antibody deposits are prominent at the NoR of distal intramuscular axons, as illustrated here by co-localisation with the nodal and paranodal marker, pan-neurofascin antibody (Fig. 1A). The juxta-terminal NoR bear the most prominent antibody deposits; thus the fluorescence intensity of anti-GD1a antibody deposits observed at NoR decreases with increasing distance from the nerve terminal. In order to quantitatively assess this, intramuscular nerve bundles were categorised into 3 groups (Fig. 1B). The single arrow indicates a single fibre; double arrow a small bundle (<15µm); and triple arrow a medium bundle (15-35µm). A further category of large nerve bundles was assigned for bundle diameters exceeding 35µm; this category is not shown in Fig. 1B as none were evident in this distal area of the intramuscular nerve complex. Anti-GD1a antibody applied to TS muscle preparations *ex vivo* were deposited at significantly higher levels at single fibre NoR compared to all other bundle categories and control tissue (Fig. 1C, D; *P*<0.001). This was also evident

for small bundles (*P*<0.001) and medium bundles (*P*=0.0023). Large bundles had an insignificant anti-GD1a antibody deposition level, comparable to control tissue, suggesting anti-GD1a antibody was unable to gain access to bundles of this size following topical application. In order to assess anti-GD1a antibody penetration to these intramuscular nerve compartments when delivered through the vascular bed (as opposed to organ bath incubation), anti-GD1a antibody was injected intraperitoneally, and 16 hours later the TS muscle was removed for antibody quantification, as for *ex vivo* preparations above. Equivalent results to the *ex vivo* findings were observed, with antibody deposits being greatest in the distal part of the nerve in a gradient-dependent manner when categorised by bundle size (Fig. 1E). In order to establish that these differences were not due to a proximal to distal gradient of GD1a expression at NoR in nerve, frozen sections of permeabilised intramuscular nerve bundles in which antibody access is expected to be uniform were stained with anti-GD1a antibody, and the signal intensity was found to be the same, irrespective of the nerve bundle size (Fig. S4). These *ex vivo* and *in vivo* findings demonstrate that anti-GD1a antibody is able to bind to intramuscular nerve NoR in a distal to proximal downward gradient, presumed due to the relatively increasing impermeability of the BNB to antibody as bundle size increases.

Nodal proteins are disrupted and distal motor nerves are rendered inexcitable by anti-GD1a antibody directed complement activation

In our previously reported model of anti-ganglioside mediated injury to the nerve terminal, complement activation has been monitored by heterologous (human) MAC deposition at motor nerve terminals (Plomp and Willison2009). Similarly in this study, MAC deposition was demonstrated at NoR of the distal intramuscular nerves in response to the addition of an exogenous source of human complement in the form of NHS (Fig. 2A). As with anti-GD1a antibody deposition, MAC deposition as assessed by fluorescence intensity for anti-MAC antibody was gradient-dependent, with significantly higher levels of fluorescence observed at single fibre NoR compared to all other categories (Fig. 2B; $P<0.001$) and significantly higher MAC levels at small bundle NoR compared to larger categories (Fig. 2B; $P<0.001$). Axonal injury was further characterised by the complete loss of the endogenous axonal CFP signal, both at the nerve terminal and along the distal axon as illustrated in Fig. 2C. Even in large bundles, the CFP signal was relatively attenuated in antibody plus NHS treated preparations.

In order to assess the functional effect of MAC deposition to the distal axonal region, electrophysiological assessment of local ion currents was performed by recording perineural currents. End plate microelectrode recordings would not be useful to assess this as all our previous electrophysiological studies have shown that the motor nerve terminal is irreversibly paralysed in this model (Plomp and Willison, 2009). Perineural recordings were made at the nerve terminal, at small nerve bundles and at large nerve bundles. In control tissue (anti-GD1a antibody without NHS), biphasic waveforms (see discussion for a fuller account of the nature of the waveform) were observed that correspond to

currents flowing through Na^+ and K^+ channels respectively (Fig. 2D, top panels). After treatment of tissue with anti-GD1a antibody plus NHS as a complement source, there was a complete loss of both K^+ (broken arrow) and Na^+ (solid arrow) current flow at the nerve terminal and nerve bundles, with the exception of preserved Na^+ current in large bundles (Fig. 2D, lower panel, arrow).

To investigate the structural correlate of this complement-associated loss of function, the architecture of the NoR was investigated by analysing the nodal appearance under phase microscopy and by immunostaining for NoR proteins located at various nodal sub-domains under injurious conditions. Electron microscopy of the NoR was also conducted; however the control tissue, having been exposed to organ bath conditions for ~5hours prior to fixation showed significant artefactual abnormalities, rendering this method assessment of any additional pathology at the experimentally injured NoR inappropriate. The percentage of NoR with intact staining for NaV1.6, the sodium channel isoform expressed at the peripheral nerve NoR (Caldwell *et al.*, 2000) was reduced (<90%) in single fibres and small bundles after treatment, compared to control (Fig. 3A; *P*<0.001). The cytoskeletal protein ankyrin G was similarly affected (Fig. 3B; *P*<0.001), as was the paranodal axolemmal protein Caspr (Fig. 3C; *P*<0.001). Staining for neurofascin was partially lost at single fibre and small bundle NoR (Fig. 3D; *P*<0.001 and *P*=0.001, respectively), and at NoR where it was preserved, the pattern was disrupted. Immunostaining to the potassium channel Kv1.1 localised to the juxtaparanode was unaffected in all bundle categories (Fig. 3E).

The complete and rapid disappearance of key NoR component proteins as assessed by immunostaining following 3hrs of NHS exposure was striking. In order to assess this in more detail for Nav1.6, intermediate stages of dissolution of Nav1.6 immunostaining were qualitatively examined at 15mins and 30mins after the addition of complement treatment. At 15min there was no alteration to staining; however by 30mins a proportion of NoR developed punctuate and dispersed Nav1.6 staining, indicating fragmentation and spread of Nav1.6 channel clusters bound by the anti-Nav1.6 antibody, examples for 3 separate NoR being shown in Fig. S5.

In this model, the motor nerve terminal is also severely and concomitantly injured such that it might conceivably have more proximal motor axonal consequences. By way of control to ensure that the observed nodal protein staining loss was associated with MAC deposition and injury directly at the NoR, Nav1.6 staining at NoR was assessed after α-LTx-induced injury that creates a nerve terminal lesion identical to that of anti-GD1a antibody directed MAC (Fig. S6). Nav1.6 immunostaining was still intact after LTx treatment, thereby confirming that its loss is due to anti-GD1a antibody with local complement activation at NoR. Taken together these results suggest that anti-GD1a antibody directed complement-mediated disruption to the nodal architecture of the distal axons results in a block in nerve conduction.

Complement inhibition completely protects nodes of Ranvier from anti-GD1a antibody-mediated injury

In order to demonstrate the role for the MAC component of complement activation, the C5 complement inhibitor Eculizumab, that completely prevents MAC assembly, was introduced to the organ bath model. Eculizumab protected Nav1.6, ankyrin G and Caspr immunostaining at NoR from injury mediated by complement activation, compared with the isotype control antibody ALXN3300. In quantitative analysis, the percentage of NoR with intact Nav1.6 staining is significantly greater on the addition of Eculizumab compared to the isotype-matched control mAb ALXN3300 at single fibres and small bundles (Fig. 4A; *P*<0.001). As demonstrated previously, there was no reduction in immunostaining at medium and large bundles in response to complement and thus complement inhibition could not further attenuate this. Single fibre and small bundle NoR also had significantly preserved ankyrin G and Caspr staining with Eculizumab protection compared to ALXN3300 application (Fig. 4B,C; *P*<0.001). Additionally, endogenous CFP was maintained in axons and bundles with Eculizumab treatment compared to ALXN3300, essentially maintaining the normal overall architecture with a normal appearance (Fig. 4D).

Calpain inhibition protects Na channel and axonal protein integrity without preserving nerve currents

A major consequence of MAC pore deposition in plasma membranes is the formation of a bi-directional, non-specific ion and water pore. At the NoR, the electrical function of the nodal axolemmal membrane is dependent upon tightly regulated ion homeostasis and the consequences of this uncontrolled flux are

likely to be considerably detrimental. One harmful ion flux mediated by MAC pores is the calcium ingress that activates calpain. To assess the consequence of the calcium component of ion influx, the protective effect of the synthetic calpain inhibitor AK295 was investigated. Neurofilament is a known calpain substrate (Chan and Mattson 1999) and its protection by calpain inhibition in response to anti-ganglioside antibody-mediated complement-dependent injury has been reported previously in our nerve terminal mouse model of GBS (O'Hanlon et al.,2003). In the present study, neurofilament at the NMJ was also significantly protected by 100μm AK295 treatment compared to antibody and NHS treated, AK295 unprotected tissue (Fig. 5).

At the NoR in *ex vivo* whole-mount TS muscle preparations exposed to antibody and NHS with and without AK295, assessments of Nav1.6, ankyrin G and Caspr immunostaining, and of perineural electrophysiological recordings were made. As expected, the extent of MAC deposition at NoR was completely unaffected by AK295 (data not shown). Nav1.6 immunostaining at single fibre and small bundle NoR was almost completely protected by AK295 treatment compared to unprotected treated muscle (Fig. 6A; $P<0.001$). Ankyrin G and Caspr immunostaining was equally protected by calpain inhibition at single fibre and small bundle NoR (Fig. 6B,C; $P<0.001$). For all nodal markers, the staining at NoR in medium and large bundles did not significantly differ as injury does not occur at these more proximal NoR.

To functionally assess the protective properties of AK295, perineural recordings were conducted as previously Fig. 6D. Compared to normal control

tissue currents, perineural Na$^+$ and K$^+$ currents were adversely affected by anti-GD1a antibody plus NHS, despite the presence of AK295. Thus, a similar loss of current flow to that seen in injured tissue as shown in Fig. 2D (lower panel) was observed. These data indicate that calpain inhibition is able to prevent the destruction of major structural components at NoR, included Nav1.6 channels, but that despite this, loss of nodal conduction as assessed electrophysiologically still occurs.

Nodes of Ranvier in the nerve trunks are also vulnerable to anti-GD1a antibody and MAC-mediated calpain activation

Whilst distal intramuscular nerve NoRs were the predominant target site investigated in this study, more proximal nerve trunks were also studied for vulnerability to anti-GD1a antibody mediated attack. The aims of examining nerve trunks were several-fold: a) to exclude the possibility that the vulnerability to anti-GD1a antibody-mediated injury was due to a distal to proximal GD1a antigen gradient in nerves (rather than a reflection of antibody access); b) to exclude the possibility that concomitant, latrotoxin-like nerve terminal injury was responsible for any disruption to the juxta-terminal NoRs examined in nerve-muscle preparations; c) to assess any distinction between motor and sensory nerve vulnerability; and d) to provide additional electrophysiological evidence in support of the perineural recording data through CAP recordings in nerve bundles. Experiments on nerve trunks were conducted with anti-GD1a antibody

and NHS as the complement source, in the presence and absence of calpain inhibition with AK295.

Preliminary studies were conducted on desheathed sciatic nerve that contains both motor and sensory fibres, chosen for its ease of dissection and widely recognised applicability to CAP measurement in recording chambers. Control nerves were compared with antibody and complement treated nerves (see materials and methods). In sciatic nerve, anti-GD1a and complement deposits were observed widely and significantly at NoR, but with some variation in complement fixation product within bundles and from fascicle to fascicle (data not shown). CAP recordings, expressed as a percentage of starting values, showed only a modest reduction in amplitude in treated nerves (87.3 ± 16%) compared with control nerves (109 ± 5.3%) which was not significant (paired t-test, p=0.2). Illustrative traces are shown in Fig S7 panel A.

Subsequently a predominantly motor nerve (phrenic; 70% of myelinated fibres being motor, Langford and Schmidt 1983) and purely sensory nerve (sural) were investigated in parallel, one advantage being that these nerves could remain in the recording chamber throughout the experimental incubations with NHS as the complement source, and continuous serial recordings could thus be collected, followed by end-point immunohistology. Anti-GD1a antibody and complement (MAC) deposition was present at NoR in both phrenic and sural nerve; however their appearance was significantly different, being more elongated in distribution across the NoR in phrenic nerve compared to sural nerve (Fig. 7A), an observation that could be readily quantitated (Fig. 7B;

P<0.001) . Furthermore, sural nerve NoRs with antibody and MAC deposits and yet intact Nav1.6 channel immunostaining was often observed (Fig. 7C), a finding not seen in the phrenic nerve or its intramuscular branches. In terms of functional effects on CAP amplitudes, sural nerve CAPs remained stable or only modestly reduced over time (76.3 ± 9.6%; Fig S7 panel B), which was not significantly different from controls.

In phrenic nerves, immunostaining of Nav1.6, ankyrin G and Caspr at NoR was quantified in response to anti-GD1a and NHS exposure. Having demonstrated nodal protein loss upon NHS exposure, experiments were also conducted in the presence and absence of AK295 (calpain inhibition) as for the *ex vivo* TS preparation. Immunostaining of the extracellular domain of NrCAM, and moesin (a Schwann cell microvillal component) was also assessed, these being molecules within the nodal complex but predicted to be unaffected by calpain cleavage directly (Fig. S8). There was a significant loss of immunostaining to Nav1.6, ankyrin G and Caspr in nerve exposed to antibody and complement, compared to control (Fig. 8A, C; *P*<0.001). Unlike the reduction in Nav1.6, ankyrin G and Caspr staining, the NrCAM and moesin staining was retained but appeared mislocalised, being more diffusely spread throughout the NoR area in comparison with the staining pattern in control tissue (Fig. 8A, C).

Nav1.6 channel and Caspr staining was significantly protected by AK295 (Fig 8B; *P*=0.01 for both proteins), although this was more modest when compared with the levels of protection achieved at the distal nerve NoR. Protection of ankyrin G staining followed the same trend but did not achieve

significance (P=0.14). The retained but disrupted pattern of NrCAM and moesin immunostaining was not altered by AK295 treatment.

Under phase optics (differential interference contrast, DIC), a constant feature observed in phrenic nerve subjected to MAC deposition and injury was the swollen, granular appearance of the NoR, in comparison with control tissue, as visible in images (Fig. 8C). This subjective and unquantifiable appearance was unaffected by AK295 treatment (Fig 8C, top row) but was consitently present. 2 examples of each antibody staining pattern are shown for AK295 protected NoR (Fig 8C, R hand panels). Extracellular recordings of phrenic nerve CAPs showed a large fall in amplitude over time (to 40.5 ± 10.7%) after treatment with anti-GD1a antibody and complement, in comparison with peak amplitude of the CAP prior to complement exposure. (Fig 8D, E). This fall in CAP amplitude was not significantly prevented by AK295 treatment (15.0 ± 8.7%, P=0.3).

Discussion

This study presents 3 major findings that develop our knowledge of nerve injury in anti-GD1a ganglioside antibody-mediated acute neuropathy models. Firstly, we demonstrate the increased vulnerability of very distal intramuscular NoR to antibody and complement mediated injury, in comparison with more proximal nodes that are relatively protected by the blood nerve barrier. Secondly, we show that axolemmal MAC pores at NoR result in calpain activation that in turn causes a) immunodetectable loss of key protein components of the nodal complex including Nav1.6 channels, most likely by protein cleavage leading to fragmentation (Iwata *et al.*, 2003, von Reyn *et al.*, 2009), and b) loss of function as demonstrated by the inability to record nerve terminal action potentials in distal axons. Implicit in the inhibition studies that demonstrated the involvement of complement and calpain activation, we infer that blockade of these pathological processes could be exploited therapeutically. Thirdly, we show that electrical inexcitability of the NoR induced by MAC pores can occur in the presence of preserved gross structural integrity including that of key protein components (Nav1.6, ankyrin, Caspr), suggesting that failure of the axolemmal membrane to maintain ionic homeostasis when punctured by MAC pores is the critical factor in mediating axonal conduction block in this model.

The study has been facilitated by new investigative approaches. Firstly, we established that intramuscular motor nerve NoR provide a simple site

relatively devoid of blood nerve barrier restrictions for analysing the pathological effects of locally or systemically delivered autoantibodies that might target this site, both *ex vivo* and *in vivo* (Burkel1967; Malmgren and Olsson1980; Olsson1990). As part of this we mapped the antibody access gradient in intramuscular nerve bundles, allowing us to identify and focus attention on the most vulnerable distal sites. We also demonstrated that any distal NoR effects did not result from concomitant latrotoxin-like, pre-synaptic injury that occurs in this model (Duchen *et al.,* 1981;Plomp and Willison, 2009). A particular advantage of this preparation is that it allows for concomitant experimentation on neuromuscular junctions and NoR, although the former site was not assessed in this study as it has been previously addressed (Goodfellow *et al.*, 2005). Secondly we have exploited genetically modified mice in which ganglioside antigen (and consequentially antibody binding) levels can be controlled, crossed with constitutive fluorescence for easy identification of intramuscular axons (Feng *et al.*, 2000; Okada *et al.*, 2002). The development of mouse models that display structural and functional similarities to the disease process in humans is an important goal for understanding mechanism and therapies. Models have limitations, in that only restricted elements of the human pathological cascade are monitored under very controlled conditions; however this also provides opportunities for unique insights into pathogenesis as highly selected events can be tracked in their entirety. Thus in this study we have precisely established the nature of acute pathological and electrophysiological events that result from MAC

injury to NoR and their therapeutic responsiveness, events that would never be tractable either in man or in longer term *in vivo* animal studies.

The application of perineural recordings to electrophysiologically monitor NoR in our studies was also critical as we know from extensive prior work that the motor end plate is concomitantly paralysed in this model, and as a result measurement of endplate potentials or muscle action potentials was not a viable means to indirectly assess NoR function. The size and location of nerve terminals at mammalian motor neuromuscular junctions has made it a huge technical challenge to employ conventional intracellular or patch clamp recording techniques to directly record the electrical activity of neurons. However, the perineural recording technique allows for the recording of local electrical signals, resulting from the opening of ion channel from the preterminal, terminal and axonal regions of motor neurons (Brigant and Mallart, 1982 Mallart, 1985). When an electrode is inserted through the perineural sheath of a motor nerve close to nerve terminals a waveform composed of two negative spikes can be recorded upon nerve stimulation. The first negative spike is attributed with inward Na^+ current (sensitive to TTX) at the nodes of Ranvier in the axonal trunk, and the second negative spike represents the net local circuit current generated by the large outward current of K^+ and a relatively small inward Ca^{2+} current at motor nerve terminals. By convention the first negative deflection is referred to as a Na^+ current (I_{Na}) and the second negative deflection is a K^+ current (I_K).

The loss of recordable perineural currents in a distal-dominant pattern correlated well with our immunohistological findings. At the distal NoR, the

absence of recordable currents indicates a severe disruption of the ability of the NoR and motor nerve terminal to generate Na^+ and K^+ currents respectively. This may either be due to calpain cleavage of the channels directly, or due to the inability of the injured axon to maintain a resting membrane potential in the presence of MAC pores. The perineural current data obtained in the presence of calpain, in which channel integrity is preserved, indicate the latter mechanism is more likely, as discussed further below. In the large intramuscular nerve bundles which are relatively resistant to injury, we found the Na^+ current to be relatively preserved whereas the K^+ current was reduced or absent, and interpreted this as an inability to generate or propagate an action potential in the severely affected distal motor nerve that would be required to activate the terminal's voltage dependent K^+ channels. Even though antibody and complement levels were undetectable in large intramuscular bundles, the attenuation of the CFP signal in these bundles (as seen in Figure 2C) suggests that some level of injury with resultant CFP leakage is taking place, but at an insufficient level to ablate either the Nav1.6 immunohistology signal, or the perineural Na^+ current. Whilst these explanations derive from current recording data that is indirectly linked to specific channel function, they nevertheless offer an internally consistent interpretation of our observations and are also consistent with our previous experiments in which mono-phasic waveforms (Na^+ current) result from loss of sodium channel function with apparent block of the K^+ current (Braga *et al.*, 1992).

Our previous studies have shown that the nerve terminal in this mouse model of anti-GD1a antibody-mediated AMAN is dependent upon MAC

deposition (Goodfellow *et al.*, 2005; Willison *et al.*, 2008), and can be completely attenuated by the C5 neutralising antibody, Eculizumab (Halstead *et al.*, 2008b) . Here we also demonstrate the pivotal role for complement in mediating the disorganisation of the NoR, and its inhibition by Eculizumab, thereby supporting our previous work. This also supports data from an active immunisation model of AMAN in rabbits in which ventral root NoR are targeted by anti-GM1 antibody and complement that can be inhibited by Nefomstat mesilate, although the precise mechanism(s) underlying this protection may be different (Phongsisay *et al.*, 2008). This raises the therapeutic prospect of using Eculizumab in AMAN and GBS patients, as has been achieved in other MAC mediated disorders (Hillmen *et al.,* 2006).

The MAC pore, like many other pore forming toxins, comprises a transmembrane doughnut-shaped channel of ~5nm pore size that allows unselective, bidirectional flow of water, ions and soluble intracellular constituents (Podack *et al.*, 1982; Lacovache *et al.,* 2008) including CFP. Thus in this model, the outward flow of CFP and its subsequent dilution in the extracellular environment (accounting for its disappearance; it is not a calpain substrate) appears to be a very sensitive marker of pore formation. Even in the large intramuscular nerve bundles in which MAC is undetectable, the CFP signal is attenuated, although this may alternatively be due to diffusion down axon with subsequent leakage in the more distally injured region.

At the NoR under physiological conditions in which it is bathed in extracellular fluid, or exposed to Ringer's (containing 2mM Ca^{2+} as present in our

ex vivo preparations), extracellular Ca^{2+} will flow intracellularly through MAC pores where one effect will be to activate the ubiquitous family of calcium activated cysteine proteases, or calpains, as we have previously shown for the nerve terminal (O'Hanlon *et al.*, 2003). Calpain-mediated proteolysis cleaves a wide range cytoskeletal and membrane proteins (Vosler *et al.,* 2008), and the protective consequence of its pharmacological inhibition provides the evidence of its activation, as demonstrated here. Ankyrin G and neurofilament proteins are long known calpain substrates and more recent *in vitro* studies have also identified the sodium channel as a calpain substrate (Iwata *et al.,* 2004; von Reyn *et al.,* 2009). Our finding of Nav1.6 protection by calpain inhibition, as demonstrated by preserved immunostaining, supports these reports. Both of the Nav.1.6 antibodies we used (see Table 1) bind to peptide domains on calpain-susceptible intracellular cytoplasmic loops between transmembrane channel subunits. Thus, the apparent 'disappearance' of Nav1.6 observed in this study over such a short timeframe most likely equate to cleavage of the cytoplasmic loop(s), rather than a more global disintegration, internalisation, or shedding of Nav1.6. Moreover, proteolysis of Nav1.6 intracellular loops may not majorly affect channel function, since activation is preserved, the dominant effect being a failure of inactivation (von Reyn et al 2009). Since ankyrin G links Nav1.6 to the cytoskeleton, it is equally possible that the un-tethered Nav1.6 becomes mislocalised through lateral diffusion; indeed multiple effects of MAC-mediated injury are likely. Our attempts to identify channel fragments by Western blotting were unsuccessful, owing to the minute amounts of Nav1.6 protein fragments in

either phrenic nerve or neuromuscular preparations (data not shown). The mislocalised but preserved immunostaining of Kv1.1 at the juxtaparanode, moesin in the Schwann cell microvilli, and the extracellular domain of NrCAM at the NoR, alongside the phase optics images of the NoR, strongly suggests that highly selective injury to the NoR axolemma was accompanied by local swelling and disorganisation, with grossly preserved structural integrity of the glial-axonal unit over this timeframe. The mechanistic similarities between this model and the Nav1.6 loss at ventral root NoR recently reported in the more chronic rabbit model of anti-GM1 antibody-mediated AMAN are intriguing, but unknown (Susuki et al., 2007b) .

Functional performance of the NoR under these injurious conditions was assessed with particular attention to Nav1.6, owing to its central role in nodal conduction. Injured NoR rapidly became electrically inactive, even when Nav1.6 and other calpain substrates were protected by AK295 treatment; indicating that failure to maintain ionic and water homeostasis owing to the presence of MAC pores, leading to membrane depolarization and inactivation of Nav1.6 channels, was the most likely mechanism, rather than Nav1.6 disruption. Similar conclusions were drawn following our studies at the nerve terminal in which the calpain inhibitor calpeptin was ineffective at protecting function or ultrastructure, although the neurofilament integrity was preserved (O'Hanlon *et al.*, 2003). Ideally, ultrastructural examination of NoR would inform this; however electron micrographs of both control and affected NoR all showed fixation-related artefacts owing to the extended periods of time the nerve was maintained *ex*

vivo, and were not suitable for analysis. In the previously reported rabbit model of AMAN, ultrastructural examination of the NoR demonstrated the extension of the nodal gap and the detachment of paranodal loops although these images were collected after a more prolonged period of injury, as noted above (Susuki *et al.*, 2007b).

Our experimental transition in this study from intramuscular nerve bundles to nerve trunks provided comparable and supportive immunohistological and electrophysiological evidence. It also unearthed a differential sensitivity of motor (phrenic) and sensory (sural) nerves to MAC mediated injury that remains unexplained. Whether this quantitative or qualitative resistance of sural nerve to MAC-mediated injury provides insights into human AMAN, in which motor nerves are selectively affected, is unknown. In the currently used GD3s$^{-/-}$ mouse model, the sural nerve contains GD1a that is sufficiently available for antibody binding with complement activation, whereas in man the levels of GD1a available for antibody targeting is most likely greater in human motor than sensory nerve (De Angelis *et al.*, 2001; Gong *et al.*, 2002).

The above model describing very distal injury as a feature of AMAN corresponds well with existing clinical data, notwithstanding the co-occurrence in some cases of severe proximal injury (Ho *et al.*, 1997; McKhann *et al.,* 1991). In terms of underlying molecular mechanisms, the acute and severe motor NoR injury in this model may correspond to the initial phases of axonal conduction block seen in human AMAN, in which rapid onset but potentially reversible pathophysiology develops, prior to any cellular infiltration or axonal degeneration.

The extent to which such events occur in man cannot be readily determined at a pathophysiological level as clinical and electrophysiological interrogation is very limited; however recovery in AMAN may be either very rapid and complete, or very prolonged with poor outcome, owing to extensive proximal axonal degeneration (McKhann *et al.*, 1993; Hiraga *et al.*, 2005b). The events at the NoR described here would correspond well with the early injury phase of a dichotomous outcome model (Gabriel 2005). Critically, inhibition of the terminal complement product, MAC, as an early intervention seems essential from these data to limiting both acute injury, and the development of more destructive long term pathology, whilst the inhibition of calpain activation downstream from MAC may also offer some partially additive benefit. The expectation that clinical trials of complement or calpain inhibition in GBS and its variants will inform this further is considerable (Wang *et al.*, 2004; Halstead *et al.,* 2005; Halstead *et al.,* 2008a; Halstead *et al.*, 2008b).

Figure legends

Fig.1

Anti-GD1a antibody is deposited at NoR in a gradient-dependent manner in distal intramuscular nerves. TS muscle was treated *ex vivo* with anti-GD1a antibody (100µg/ml for 160mins) and antibody deposits localised and quantified. **A)** Anti-GD1a antibody (magenta) binds at the NoR of distal motor axons as determined by co-localisation with neurofascin (green) and a narrowing of the endogenously expressed axonal CFP (blue). **B)** Nerve fibres and bundles were categorised by size for quantification. Single arrow, single fibre; double arrow, small bundle; triple arrow, medium bundle. **C)** Intensity of anti-GD1a antibody binding was assessed according to bundle size; image shows antibody at a single fibre NoR compared to that seen at small bundle NoR. **D)** Single fibres showed significantly higher fluorescence intensity at NoR compared to small bundles, small bundles compared to medium bundles, and medium bundles compared to large bundles. Single fibre, small bundle and large bundles NoR all had significantly increased levels compared to control (no antibody) tissue. **E)** 16hrs following injection of anti-GD1a antibody (i.p. total dose 3mg), fluorescence intensity at NoR showed the same gradient-dependent binding pattern as that seen in *ex vivo* antibody treated tissue compared to control PBS injected mice.

* $p<0.05$, compared to small, medium, large bundles and control; # $p<0.05$ compared to medium, large bundles and control; ** $p<0.05$, compared to large bundles and control. Scale bar = 20µm.

Fig. 2

Complement activation at distal nerve NoR is associated with marked attenuation of endogenous CFP and loss of perineural currents. *Ex vivo* TS preparations exposed to anti-GD1a antibody or Ringer's control, followed by 40% NHS as a source of complement, were examined for MAC deposition at NoR, the distribution of axonal CFP, and perineural current recordings. **A)** Illustrative image of a NoR in a small nerve bundle coated with MAC deposits. **B)** Quantification of MAC deposits demonstrated significantly higher levels at single fibre NoR, and small bundle NoR, compared to all other categories. **C)** Illustrative low power images of intramuscular CFP axon bundles (blue) terminating at BTx delineated NMJ (magenta) in control tissue exposed to Ringer's followed by NHS (left panel), and anti-GD1a antibody followed by NHS, the latter showing marked attenuation (right panel). **D)** Perineural recordings from control (Ringer's followed by NHS) and treated (anti-GD1a antibody followed by NHS) tissue demonstrate intact Na^+ (solid arrow) and K^+ (broken arrow) currents at nerve terminals, small bundles and large bundles in control nerves. These currents are completely attenuated in treated nerves, with the exception of the Na^+ currents in large bundles.

* $p < 0.05$, compared to small, medium, large bundles and control; # $p < 0.05$ compared to medium, large bundles and control. Scale bar = 10μm (A) and 20μm (C).

Fig. 3

Immunohistological appearance of nodal markers at the NoR of distal intramuscular nerves following exposure to anti-GD1a antibody and NHS (treated), compared with Ringer's and NHS (control). *Ex vivo* TS muscles were incubated with 100µg/ml anti-GD1a antibody and 40% NHS as a source of complement. The percentages of NoR positive for immunostaining in each bundle category for 5 nodal proteins were determined. **A-D)** Nav1.6, ankyrin G, Caspr and neurofascin immunostaining was significantly reduced at single fibre and small bundle NoR after treatment compared to controls. **E)** Kv1.1 immunostaining remained unchanged after treatment in all bundle categories. Merged illustrations are shown for control tissue; and both single and merged illustrations for treated tissue.

* $p < 0.05$, compared to control counterpart. Scale bar = 10µm.

Fig. 4

The complement inhibitor, Eculizumab neuroprotects the distal nerve NoR on treatment with anti-GD1a antibody and NHS. Eculizumab (100µg/ml) plus 40% NHS were admixed 10mins prior to addition to *ex vivo* TS muscle preparations and the protective effects on the immunostaining signal of Nav1.6 channel, ankyrin G, Caspr and endogenous axonal CFP were compared to tissue treated with anti-GD1a antibody and NHS admixed with the isotype matched control mAb ALXN3300. **A-C)** Nav1.6, ankyrin G and Caspr immunostaining was significantly preserved at single fibre and small bundle NoR following Eculizumab treatment;

illustrative images on right. * p<0.05, compared to control counterpart. Scale bar = 10µm. **D)** Illustrative low power images of intramuscular CFP axon bundles (white) in TS muscle terminating at BTx delineated NMJ (magenta) after treatment with Eculizumab (left image) or ALXN3300 (right image). The CFP signal is completely preserved by Eculizumab, but markedly attenuated with the isotype control antibody. Scale bar = 100µm.

Fig. 5

The calpain inhibitor AK295 protects neurofilament at the nerve terminal from degradation by anti-GD1a antibody and NHS exposure. *Ex vivo* TS muscle was treated with anti-GD1a antibody and NHS with or without 100µM AK295. Neurofilament immunostaining (red) intensity over the motor endplate (delineated by BTx, green) was measured and expressed as a percentage of normal levels. In the images, extensive pruning of the distal neurofilament arborisation can be seen in AK295 unprotected tissue (right), compared with protected tissue (left). * p<0.05, compared to AK295 treatment. Scale bar = 50µm.

Fig. 6

Calpain inhibition preserves immunostaining profiles of NoR proteins, without protecting conduction of distal axons after treatment with anti-GD1a antibody and NHS. *Ex vivo* TS preparations were incubated with anti-GD1a antibody and NHS with or without 100µM AK295 and its protective effect on the immunostaining of proteins quantified in different bundle categories. Perineural recordings were

performed after 3h of treatment. **A-C)** Nav1.6 channel, ankyrin G and Caspr immunostaining was significantly preserved by AK295 treatment in single fibres and small bundles compared to the same categories in AK295 unprotected tissue. Illustrative images depict intact staining to the right of the corresponding graphs. **D)** Perineural current traces show K^+ and Na^+ ion currents in nerve terminals, small bundles and large bundles from completely normal TS tissue (control, upper traces) and in tissue treated with anti-GD1a antibody, NHS and AK295. In AK295 treated preparations, no protection of perineural currents in single and small bundles is seen.

* p<0.05, compared to AK295 treatment. Scale bar =10μm.

Fig. 7

Differential anti-GD1a antibody binding at NoR in phrenic nerve (motor) and sural nerve (sensory). Phrenic nerve and sural nerve were desheathed and incubated with anti-GD1a antibody (100μg/ml for 2hrs) before the distribution of antibody across the NoR was quantitated. **A)** Illustrative images of staining profile. **B)** There was a significantly greater spread of antibody in phrenic nerve compared to sural nerve NoR. **C)** In sural nerve treated with anti-GD1a antibody plus NHS deposits of IgG and MAC were frequently seen at NoR without loss of Nav1.6 immunostaining, which was very rarely seen in either phrenic nerve or distal motor nerve NoR in TS preparations.

* p<0.05, comapred to phrenic nerve. Scale bar = 5μm.

Fig. 8

Phrenic nerve NoR immunostaining profiles of nodal proteins after exposure to anti-GD1a antibody plus NHS are partially protected by AK295. Phrenic nerve was desheathed and treated with anti-GD1a antibody or Ringer's, plus NHS, with and without AK295. and the effect on nodal protein immunostaining was quantified. **A)** Anti-GD1a antibody treated phrenic nerve has significantly less NoR that were immuno-positive for Nav1.6 channel, ankyrin G, Caspr, NrCAM and moesin than control. **B)** AK295 does not protect ankyrin G, and only modestly protects Nav1.6 channel and Caspr immunostaining from complement-mediated injury. **C)** Moesin and NrCAM staining profiles are not significantly altered in intensity after anti-GD1a antibody exposure; however they both show an abnormal distribution as highlighted in the images. Examples of normal control staining of all of the proteins (magenta) versus treated and AK295 protected nerve. Note occurrence of swollen morphology of treated nerves in DIC that is not ameliorated by AK295 treatment. **D)** Extracellular recordings of anti-GD1a antibody-treated phrenic nerve show a reduction in CAP amplitudes over time that are unaffected by AK295. Anti-GD1a antibody was added for 2 hours; subsequently NHS was added for 2 hours starting at 0 mins. Arrows indicate the addition of 5μM TTX to terminate the experiment. **E)** CAP amplitudes are expressed as the percentage of the starting value, there being no significant difference between AK295 treated or untreated nerves.

* $p < 0.05$, compared to control or AK295 counterpart. Scale bar = 5μm.

Supplementary figure legends

Fig. S1

Ganglioside biosynthesic pathway showing the structure of GD1a and the pattern of deficiency seen in GD3 synthase$^{-/-}$ mice.

Fig. S2

Anti-GD1a antibody more effectively binds nerve terminals in transgenic mice over-expressing a-series gangliosides (GD3$^{-/-}$/CFP) compared to wild type mice, as assessed by immunocytochemistry. TS muscle from both modified and WT mice were incubated with anti-GD1a antibody (red) and the fluorescence intensity of deposits measured over the NMJ, identified by BTx (green).
* $p < 0.05$, compared to wild-type (WT). Scale bar = 20μm

Fig. S3

Nerve desheathment results in a significant increase in anti-GD1a antibody deposition at NoR. Data shown for phrenic nerve.
* $p < 0.05$, desheathed nerve compared with intact nerve.

Fig. S4

GD1a is uniformly present at intramuscular nerve NoR irrespective of bundle size. In permeabilised TS preparations, anti-GD1a antibody binds equally to NoR

in single fibres, small, medium and large bundles, as assessed by immunohistology.

Fig. S5

Three examples of Nav1.6 channel immunostaining at the phrenic nerve NoR after anti-GD1a antibody exposure and 30mins treatment with NHS. Various stages of dissolution of Nav1.6 immunostaining are evident (arrows), prior to its subsequent complete disappearance.

Scale bar = 5μm

Fig. S6

Following α-LTx treatment that specifically disintegrates the nerve terminal through pore formation in the pre-synaptic membrane, Nav1.6 channel immunostaining is unaffected (arrow). * signifies the position of the now invisible nerve terminal arborisation where endogenous CFP is lost due to the α-LTx-evoked injury.

Scale bar = 20μm.

Fig. S7

Sciatic nerve and sural nerve CAP recordings show slight or no reduction respectively after treatment with anti-GD1a antibody and NHS as a source of complement. **A)** Extracellular recordings were obtained from control and treated sciatic nerve and the peak CAP plotted over time. Sciatic nerves were exposed

to NHS as the complement source prior to transfer to the recording chamber. **B)**
For sural nerve, NHS was added to the recording chamber at 0 mins. Arrows
indicate the addition of 5μM TTX to terminate the experiment.

Fig S8.

Summary cartoon showing the principal features of the pathophysiological
casdade occurring at NoR exposed to anti-GD1a antibody and complement.
MAC pores form in the axolemmal membrane at the NoR that allow sufficient
uncontrolled ingress of calcium to activate calpain, resulting in degradation of
calpain substrates including Nav1.6, neurofilament, Caspr and Ankyrin G.

Acknowledgements

References

Ang CW, Jacobs BC, Laman JD. The Guillain-Barré syndrome: a true case of molecular mimicry. Trends Immunol 2004; 25: 61-66.

Arroyo EJ, Xu YT, Zhou L *et al*. Myelinating Schwann cells determine the internodal localization of Kv1.1, Kv1.2, Kvbeta2, and Caspr. Journal of Neurocytology1999; 28: 333-47.

Aspinall GO, McDonald AG, Raju TS, Pang H, Moran AP, Penner JL. Chemical structures of the core regions of Campylobacter jejuni serotypes O:1, O:4, O:23, and O:36 lipopolysaccharides. European Journal of Biochemistry 1993; 213: 1017-27.

Bhat MA, Rios JC, Lu Y *et al*. Axon-glia interactions and the domain organization of myelinated axons requires neurexin IV/Caspr/Paranodin. Neuron.2001; 30: 369-8.

Boffey J, Odaka M, Nicoll D *et al*. Characterisation of the immunoglobulin variable region gene usage encoding the murine anti-ganglioside antibody repertoire. J.Neuroimmunol 2005; 165: 92-103.

Bowes T, Wagner ER, Boffey J *et al*. Tolerance to self gangliosides is the major factor restricting the antibody response to lipopolysaccharide core oligosaccharides in Campylobacter jejuni strains associated with Guillain-Barre syndrome. Infection & Immunity 2002; 70 :5008-18.

Boyle ME, Berglund EO, Murai KK, Weber L, Peles E, Ranscht B. Contactin orchestrates assembly of the septate-like junctions at the paranode in myelinated peripheral nerve. Neuron 2001; 30: 385-97.

Braga MF, Harvey AL, Rowan EG. Effects of tacrine, velnacrine (HP029), suronacrine (HP128), and 3,4-diaminopyridine on skeletal neuromuscular transmission in vitro. Br.J.Pharmacol 1991; 102: 909-915.

Braga MF, Anderson AJ, Harvey AL, Rowan EG. Apparent block of K+ currents in mouse motor nerve terminals by tetrodotoxin, mu-conotoxin and reduced external sodium. Br J Pharmacol 1992; 106:91-4.

Brigant J and Mallart, A. Presynaptic currents in mouse motor endings. J. Physiol., Lond 1982; 333: 619–636.

Burkel WE. The histological fine structure of perineurium. Anatomical Record 1967; 158:177-89.

Caldwell JH, Schaller KL, Lasher RS, Peles E, Levinson SR. Sodium channel Na(v)1.6 is localized at nodes of ranvier, dendrites, and synapses. Proceedings of the National Academy of Sciences of the United States of America 2000;.97: 5616-20.

Chan SL, Mattson MP. Caspase and calpain substrates: roles in synaptic plasticity and cell death. Journal of Neuroscience Research.1999; 58:167-90.

Charles P, Tait S, Faivre-Sarrailh C *et al*. Neurofascin is a glial receptor for the paranodin/Caspr-contactin axonal complex at the axoglial junction. Current Biology 2002; 12: 217-20.

Davis JQ, Lambert S, Bennett V. Molecular composition of the node of Ranvier: identification of ankyrin-binding cell adhesion molecules neurofascin (mucin+/third FNIII domain-) and NrCAM at nodal axon segments. Journal of Cell Biology 1996; 135: 1355-67.

De Angelis MV, Di Muzio A, Lupo S, Gambi D, Uncini A, Lugaresi A. Anti-GD1a antibodies from an acute motor axonal neuropathy patient selectively bind to motor nerve fiber nodes of Ranvier. Journal of Neuroimmunology 2001; 121: 79-82.

Duchen LW, Gomez S, Queiroz LS. The neuromuscular junction of the mouse after black widow spider venom. Journal of Physiology 1981; 316: 279-91.

Einheber S, Zanazzi G, Ching W *et al*. The axonal membrane protein Caspr, a homologue of neurexin IV, is a component of the septate-like paranodal junctions that assemble during myelination. Journal of Cell Biology 1997;.139:1495-506.

Feasby TE, Gilbert JJ, Brown WF *et al*. An acute axonal form of Guillain-Barre polyneuropathy. Brain 1986; 109: 1115-26.

Feng G, Mellor RH, Bernstein M *et al*. Imaging neuronal subsets in transgenic mice expressing multiple spectral variants of GFP. Neuron 2000; 28: 41-51.

Gabriel CM. Prognosis in the acute motor axonal form of Guillain-Barre syndrome. J.Neurol.Neurosurg.Psychiatry 2005; 76: 622.

Gong Y, Tagawa Y, Lunn MP *et al*. Localization of major gangliosides in the PNS: implications for immune neuropathies. Brain 2002; 125: 2491-506.

Goodfellow JA, Bowes T, Sheikh K *et al*. Overexpression of GD1a ganglioside sensitizes motor nerve terminals to anti-GD1a antibody-mediated injury in a model of acute motor axonal neuropathy. Journal of Neuroscience 2005; 25:1620-8.

Goodyear CS, O'Hanlon GM, Plomp JJ *et al*. Monoclonal antibodies raised against Guillain-Barre syndrome-associated Campylobacter jejuni lipopolysaccharides react with neuronal gangliosides and paralyze muscle-nerve preparations.[erratum appears in J Clin Invest 1999; 104:697-708.

Griffin JW, Li CY, Macko C *et al*. Early nodal changes in the acute motor axonal neuropathy pattern of the Guillain-Barre syndrome. Journal of Neurocytology 1996; 25:33-51.

Hafer-Macko C, Hsieh ST, Li CY *et al*. Acute motor axonal neuropathy: an antibody-mediated attack on axolemma. Annals of Neurology 1996; 40: 635-44.

Halstead SK, Humphreys PD, Goodfellow JA, Wagner ER, Smith RA, Willison HJ. Complement inhibition abrogates nerve terminal injury in Miller Fisher syndrome. Annals of Neurology 2005;.58: 203-10.

Halstead SK, Humphreys PD, Zitman FM, Hamer J, Plomp JJ, Willison HJ. C5 inhibitor rEV576 protects against neural injury in an in vitro mouse model of Miller Fisher syndrome. Journal of the Peripheral Nervous System 2008a; 13: 228-35.

Halstead SK, Zitman FM, Humphreys PD *et al*. Eculizumab prevents anti-ganglioside antibody-mediated neuropathy in a murine model. Brain 2008b.131: 1197-208.

Hillmen P, Young NS, Schubert J *et al*. The complement inhibitor eculizumab in paroxysmal nocturnal hemoglobinuria. New England Journal of Medicine 2006;.355:1233-43.

Hiraga A, Kuwabara S, Ogawara K *et al*. Patterns and serial changes in electrodiagnostic abnormalities of axonal Guillain-Barre syndrome. Neurology 2005a;.64: 856-60.

Hiraga A, Mori M, Ogawara K *et al*. Recovery patterns and long term prognosis for axonal Guillain-Barre syndrome. J.Neurol.Neurosurg.Psychiatry 2005b; 76: 719-722.

Ho TW, Hsieh ST, Nachamkin I *et al*. Motor nerve terminal degeneration provides a potential mechanism for rapid recovery in acute motor axonal neuropathy after Campylobacter infection. Neurology 1997;.48: 717-24.

Ho TW, Willison HJ, Nachamkin I *et al*. Anti-GD1a antibody is associated with axonal but not demyelinating forms of Guillain-Barre syndrome. Annals of Neurology 1999;.45: 168-73.

Hughes RA, Cornblath DR. Guillain-Barre syndrome. Lancet 2005; .366: 1653-66.

Iacovache I, van der Goot FG, Pernot L. Pore formation: an ancient yet complex form of attack. Biochim.Biophys.Acta 2008; 1778: 1611-1623.

Iwata A, Stys PK, Wolf JA *et al*. Traumatic axonal injury induces proteolytic cleavage of the voltage-gated sodium channels modulated by tetrodotoxin and protease inhibitors. Journal of Neuroscience 2004;.24: 4605-13.

Kordeli E, Davis J, Trapp B, Bennett V. An isoform of ankyrin is localized at nodes of Ranvier in myelinated axons of central and peripheral nerves. Journal of Cell Biology 1990; 110: 1341-52.

Kuwabara S, Ogawara K, Misawa S *et al*. Does Campylobacter jejuni infection elicit "demyelinating" Guillain-Barre syndrome. Neurology.2004; 63:529-33.

Langford LA, Schmidt RF. An electron microscopic analysis of the left phrenic nerve in the rat. Anat Rec 2002; 205: 207-13.

Ledeen RW. Ganglioside structures and distribution: are they localized at the nerve ending? Journal of Supramolecular Structure 1978; 8: 1-17.

Li Z, Ortega-Vilain AC, Patil GS *et al*. Novel peptidyl alpha-keto amide inhibitors of calpains and other cysteine proteases. Journal of Medicinal Chemistry 1996; 39: 4089-98.

Lugaresi A, Ragno M, Torrieri F, Di Guglielmo G, Fermani P, Uncini A. Acute motor axonal neuropathy with high titer IgG and IgA anti-GD1a antibodies following Campylobacter enteritis. Journal of the Neurological Sciences 1997;.147: 193-200.

Mallart A. Electric current flow inside perineural sheaths of mouse motor nerves. J. Physiol. Lond. 1985; 368: 565–575.

Malmgren LT, Olsson Y. Differences between the peripheral and the central nervous system in permeability to sodium fluorescein. Journal of Comparative Neurology. 1980; 103-107.

McKhann GM, Cornblath DR, Griffin JW *et al*. Acute motor axonal neuropathy: a frequent cause of acute flaccid paralysis in China. Annals of Neurology 1993;.33: 333-42.

McKhann GM, Cornblath DR, Ho T *et al*. Clinical and electrophysiological aspects of acute paralytic disease of children and young adults in northern China. Lancet 1991; 338: 593-7.

Menegoz M, Gaspar P, Le Bert M *et al*. Paranodin, a glycoprotein of neuronal paranodal membranes. Neuron. 1997; 319-331.

O'Hanlon GM, Humphreys PD, Goldman RS *et al*. Calpain inhibitors protect against axonal degeneration in a model of anti-ganglioside antibody-mediated motor nerve terminal injury. Brain 2003; 126: 2497-2509.

Ogawara K, Kuwabara S, Mori M, Hattori T, Koga M, Yuki N. Axonal Guillain-Barre syndrome: relation to anti-ganglioside antibodies and Campylobacter jejuni infection in Japan. Ann.Neurol. 2000; 48: 624-631.

Okada M, Itoh MM, Haraguchi M *et al.* b-series Ganglioside deficiency exhibits no definite changes in the neurogenesis and the sensitivity to Fas-mediated apoptosis but impairs regeneration of the lesioned hypoglossal nerve. Journal of Biological Chemistry 2002; 277: 1633-6.

Olsson Y. Microenvironment of the peripheral nervous system under normal and pathological conditions. (Review). Critical Reviews in Neurobiology 1990; 5: 265-311.

Peles E, Nativ M, Lustig M *et al.* Identification of a novel contactin-associated transmembrane receptor with multiple domains implicated in protein-protein interactions. EMBO Journal 1997;.16: 978-88.

Phongsisay V, Susuki K, Matsuno K *et al.* Complement inhibitor prevents disruption of sodium channel clusters in a rabbit model of Guillain-Barre syndrome. Journal of Neuroimmunology. 2008; 101-104.

Plomp JJ, Molenaar PC, O'Hanlon GM *et al.* Miller Fisher anti-GQ1b antibodies: alpha-latrotoxin-like effects on motor end plates. Ann.Neurol. 1999; 45: 189-199.

Plomp JJ, Willison HJ. Pathophysiological actions of neuropathy-related anti-ganglioside antibodies at the neuromuscular junction. J.Physiol 2009; 587: 3979-3999.

Podack ER, Muller-Eberhard HJ, Horst H, Hoppe W. Membrane attack complex of complement (MAC): three-dimensional analysis of MAC-phospholipid vesicle recombinants. J Immunol 1982; 128:2353-2357.

Poliak S, Peles E. The local differentiation of myelinated axons at nodes of Ranvier. Nature Reviews Neuroscience 2003; 4:968-80.

Rasband MN, Park EW, Zhen D *et al.* Clustering of neuronal potassium channels is independent of their interaction with PSD-95. Journal of Cell Biology 2002; 159: 663-72.

Rios JC, Melendez-Vasquez CV, Einheber S *et al.* Contactin-associated protein (Caspr) and contactin form a complex that is targeted to the paranodal junctions during myelination. Journal of Neuroscience 2000; 8354-8364.

Saito A, Zacks SI. Ultrastructure of Schwann and perineural sheaths at the mouse neuromuscular junction. Anatomical Record 1969; 164: 379-90.

Scherer SS. Molecular specializations at nodes and paranodes in peripheral nerve. Microscopy Research & Technique 1996;.34:452-61.

Sheikh KA, Deerinck TJ, Ellisman MH, Griffin JW. The distribution of ganglioside-like moieties in peripheral nerves. Brain 1999a; 122: 449-60.

Sheikh KA, Sun J, Liu Y *et al.* Mice lacking complex gangliosides develop Wallerian degeneration and myelination defects. Proceedings of the National Academy of Sciences of the United States of America 1999b;.96:7532-7.

Sheikh KA, Zhang G, Gong Y, Schnaar RL, Griffin JW. An anti-ganglioside antibody-secreting hybridoma induces neuropathy in mice. Annals of Neurology 2004; 56: 228-39.

Silajdzic E, Willison HJ, Furukawa K, Barnett SC. In vitro analysis of glial cell function in ganglioside-deficient mice. J.Neurosci.Res 2009; 87: 2467-2483.

Susuki K, Baba H, Tohyama K *et al.* Gangliosides contribute to stability of paranodal junctions and ion channel clusters in myelinated nerve fibers. Glia 2007a;.55: 746-57.

Susuki K, Nishimoto Y, Yamada M *et al.* Acute motor axonal neuropathy rabbit model: immune attack on nerve root axons. Annals of Neurology 2003; .54: 383-8.

Susuki K, Rasband MN, Tohyama K *et al.* Anti-GM1 antibodies cause complement-mediated disruption of sodium channel clusters in peripheral motor nerve fibers. Journal of Neuroscience 2007b; 27: 3956-67.

Tait S, Gunn-Moore F, Collinson JM *et al.* An oligodendrocyte cell adhesion molecule at the site of assembly of the paranodal axo-glial junction. Journal of Cell Biology 2000; 150: 657-66.

Takamiya K, Yamamoto A, Furukawa K *et al.* Mice with disrupted GM2/GD2 synthase gene lack complex gangliosides but exhibit only subtle defects in their nervous system. Proceedings of the National Academy of Sciences of the United States of America. 1996; 93: 10662-7.

Traka M, Dupree JL, Popko B, Karagogeos D. The neuronal adhesion protein TAG-1 is expressed by Schwann cells and oligodendrocytes and is localized to the juxtaparanodal region of myelinated fibers. Journal of Neuroscience 2002;.22: 3016-24.

von Reyn CR, Spaethling JM, Mesfin MN *et al*. Calpain mediates proteolysis of the voltage-gated sodium channel alpha-subunit. Journal of Neuroscience 2009;.29:10350-6.

Vosler PS, Brennan CS, Chen J. Calpain-mediated signaling mechanisms in neuronal injury and neurodegeneration. Mol.Neurobiol. 2008; 38: 78-100.

Wang H, Kunkel DD, Martin TM, Schwartzkroin PA, Tempel BL. Heteromultimeric K+ channels in terminal and juxtaparanodal regions of neurons. Nature 1993;.365: 75-9.

Wang MS, Davis AA, Culver DG, Qinbo Wang Q, Powers JC, Glass JD. Calpain Inhibition Protects against Taxol-induced Sensory Neuropathy. Brain 2004; 127: 1-9.

Willison HJ, Halstead SK, Beveridge E *et al*. The role of complement and complement regulators in mediating motor nerve terminal injury in murine models of Guillain-Barre syndrome. Journal of Neuroimmunology. 2008; 172-182.

Figure 1

Figure 2

A

B

ex vivo

C
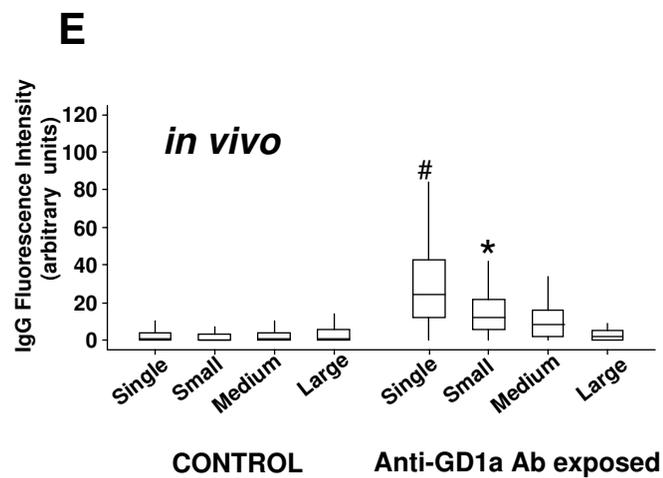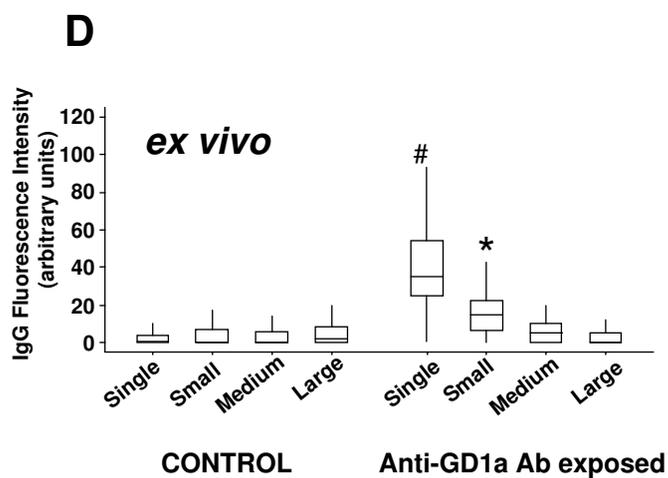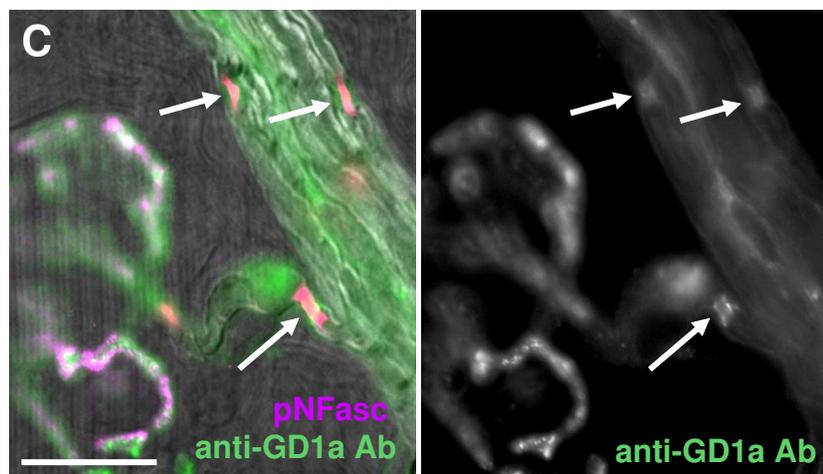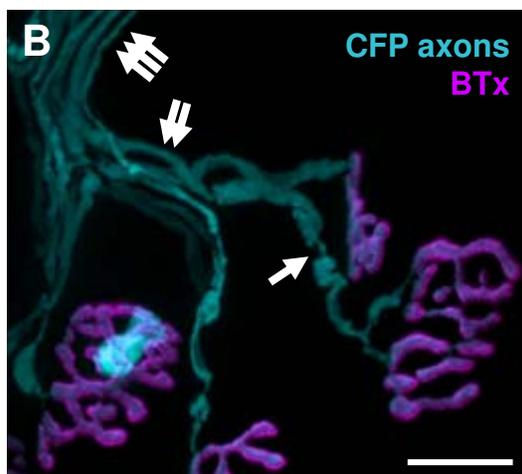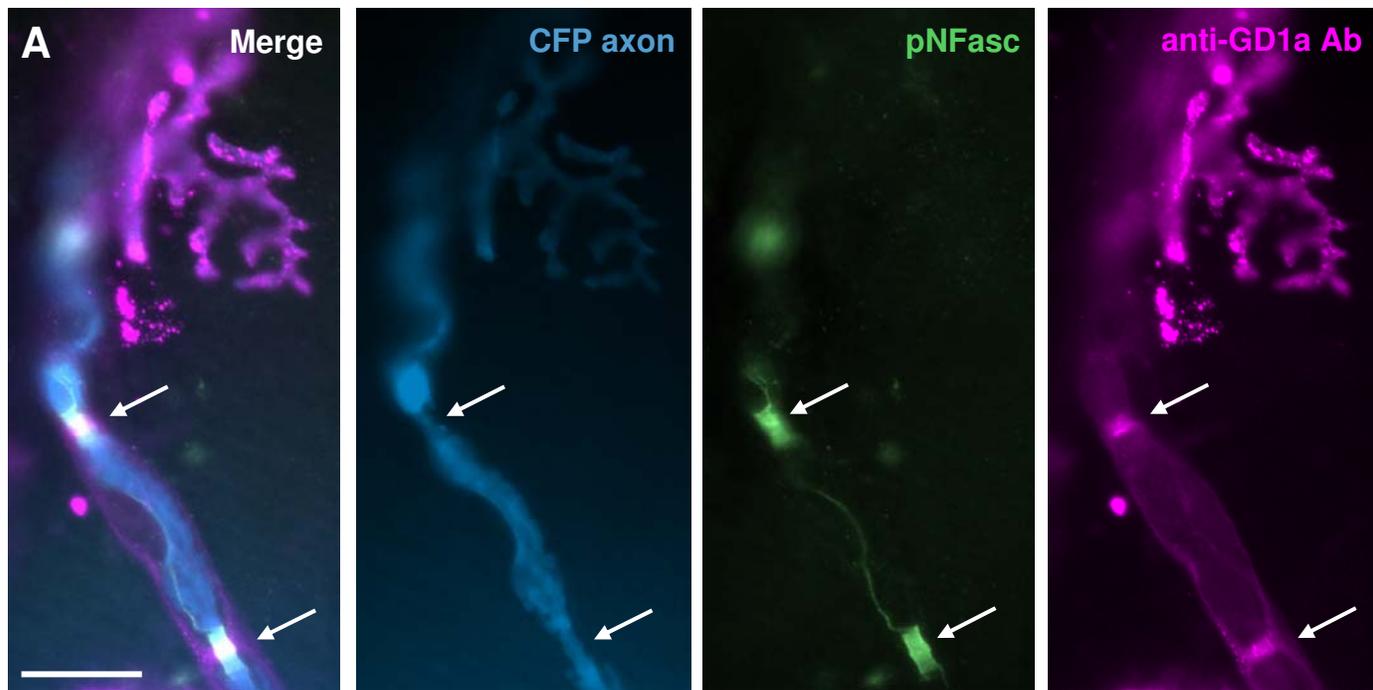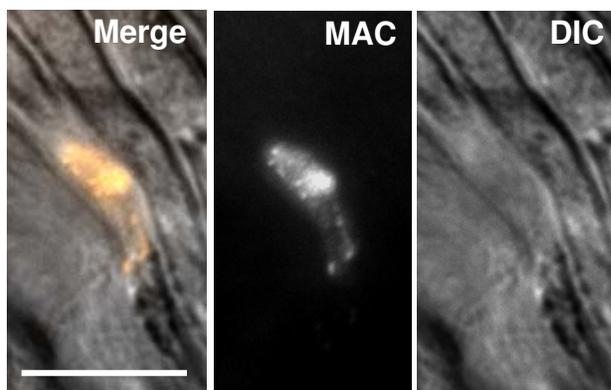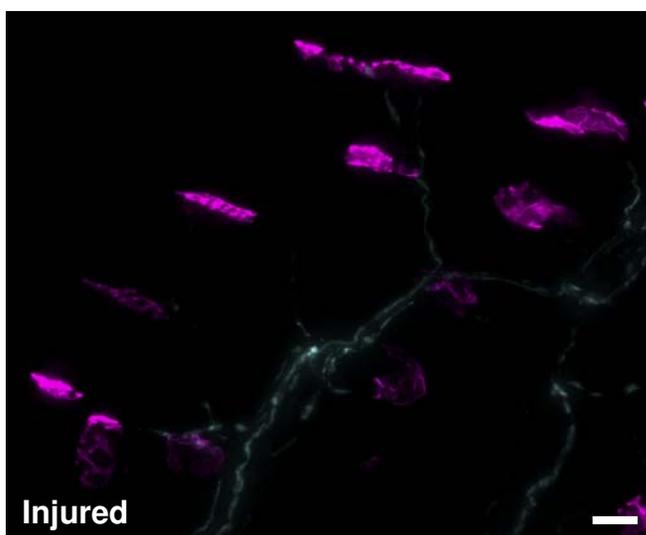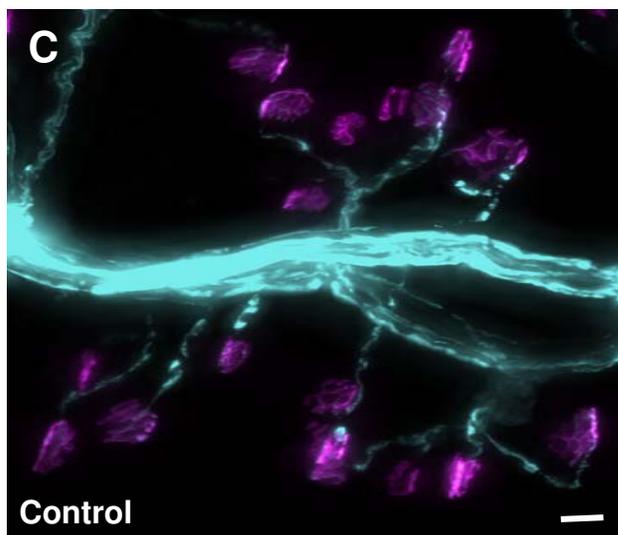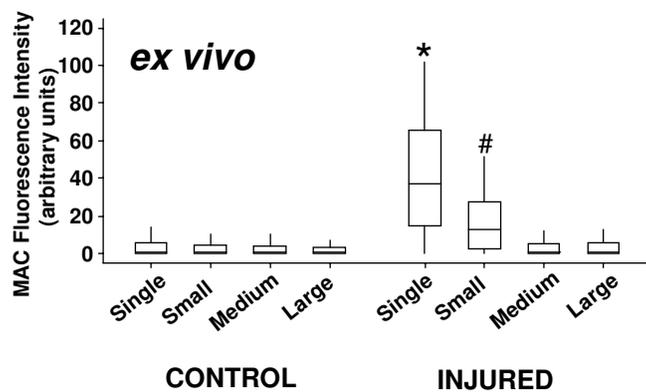
D
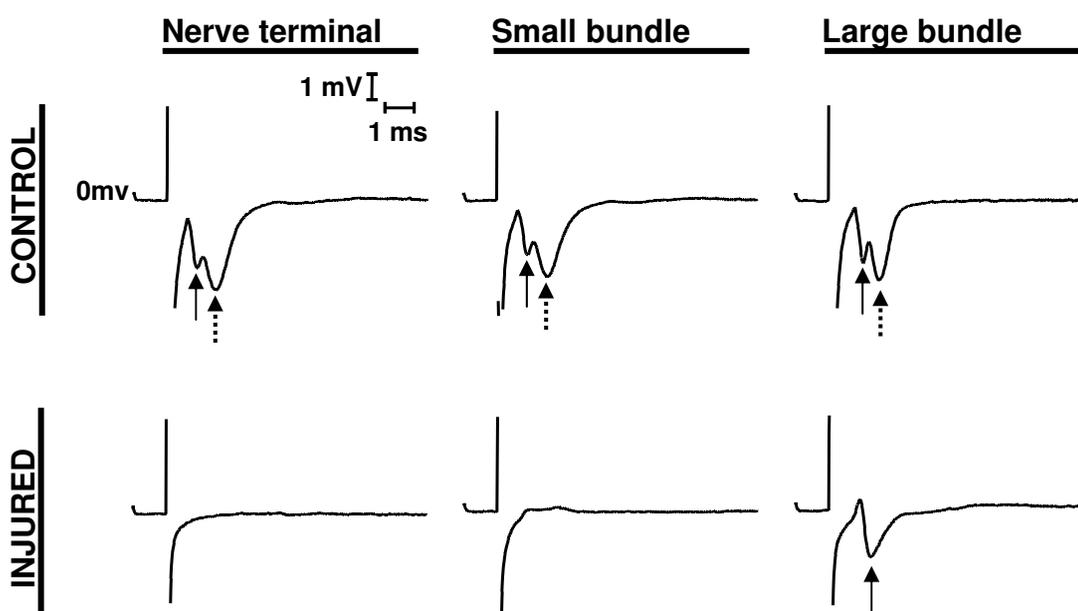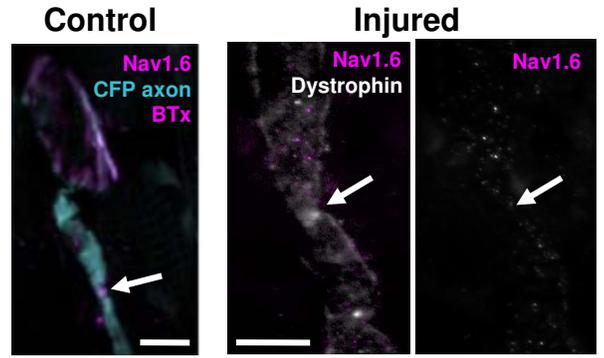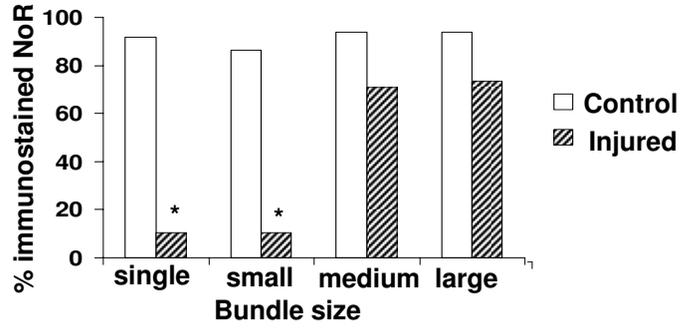
Figure 3

A Nav1.6

B Ankyrin G
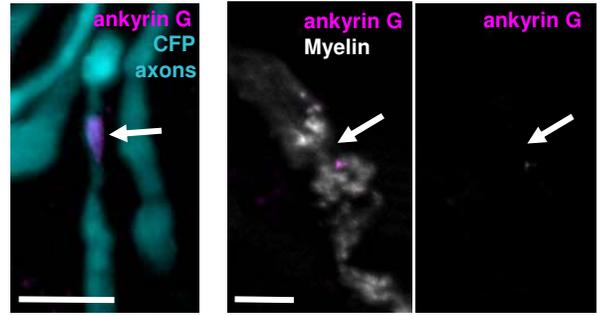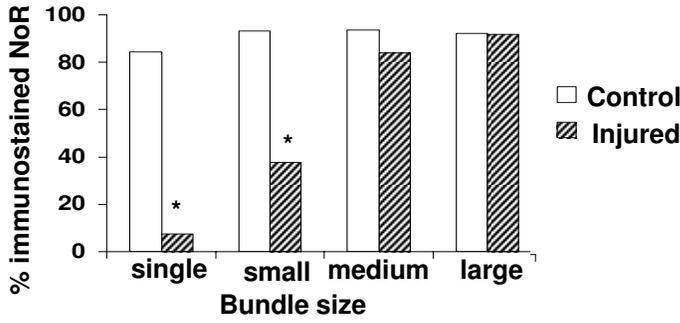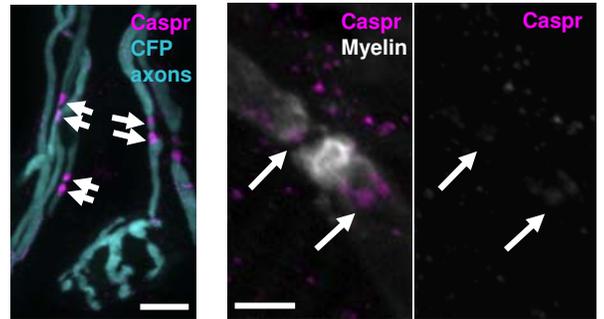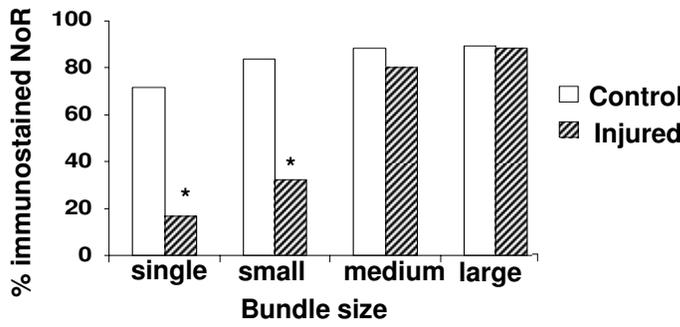
C Caspr

D pan-Neurofascin
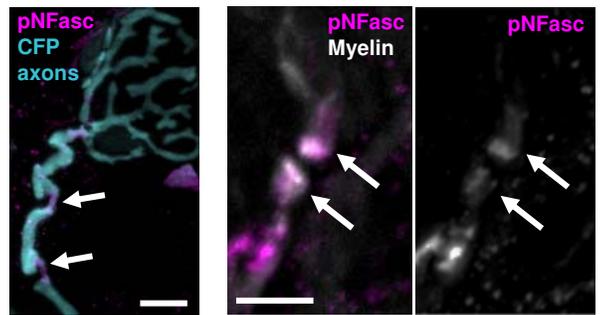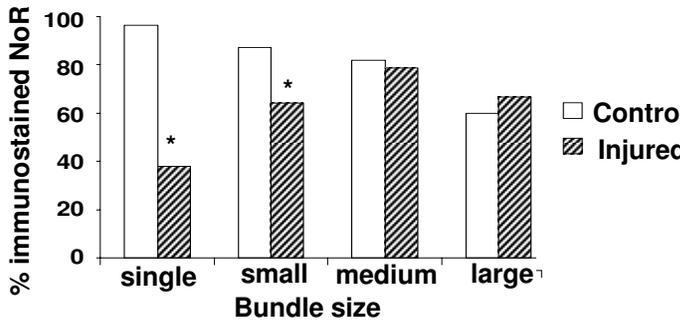
E Kv1.1
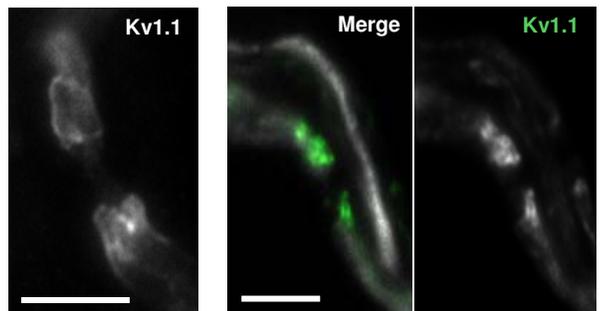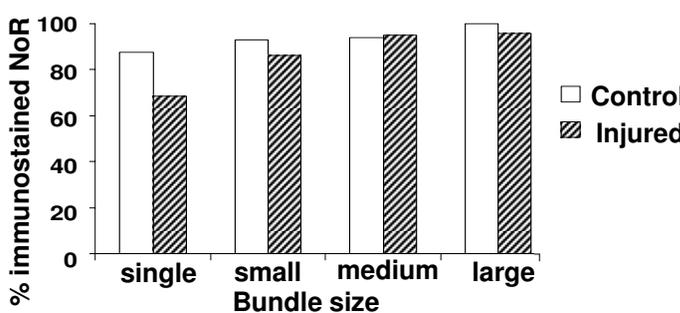
Figure 4

A Nav1.6

B Ankyrin G

C Caspr

D

Figure 5

AK295 protected

Merge

Neurofilament

AK295 unprotected

Merge

Neurofilament
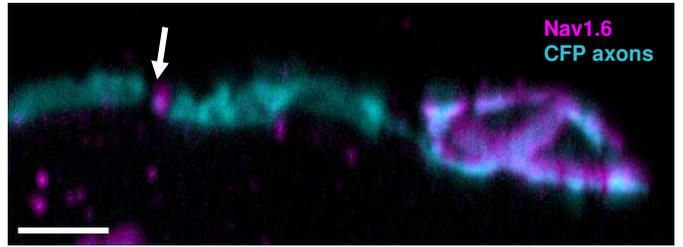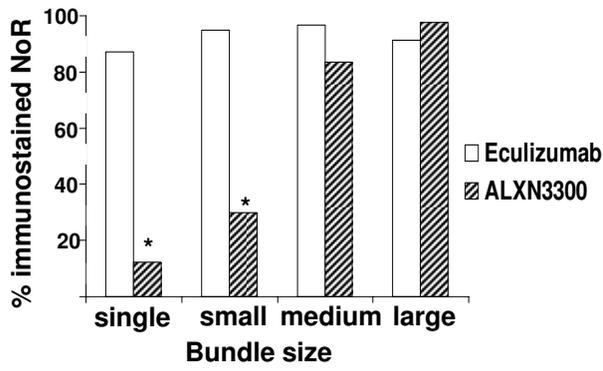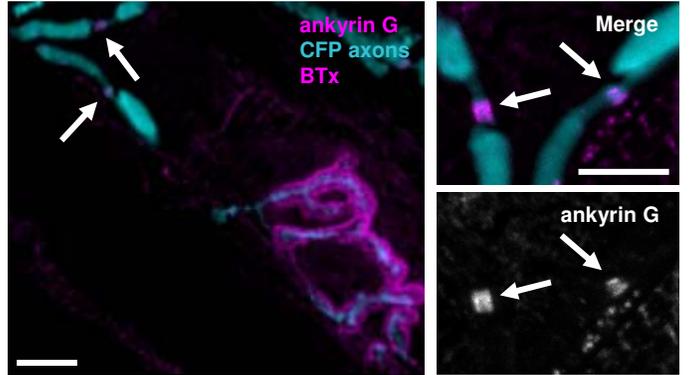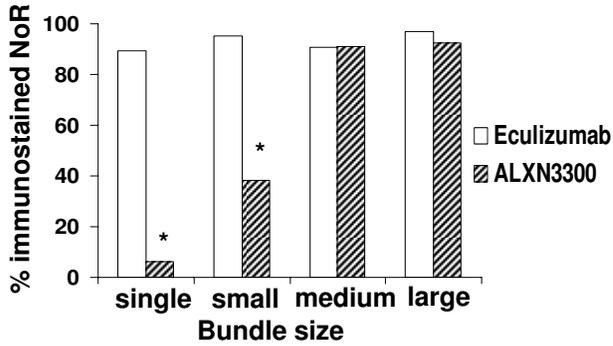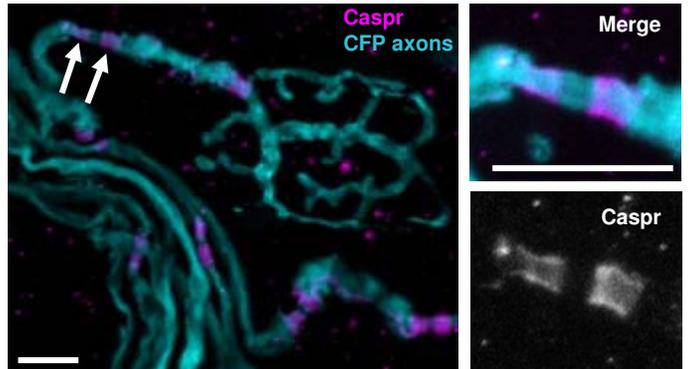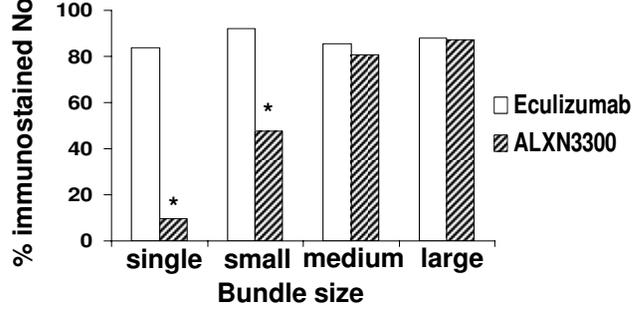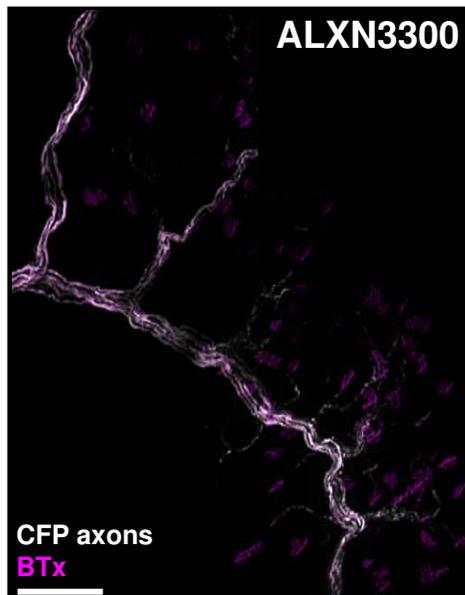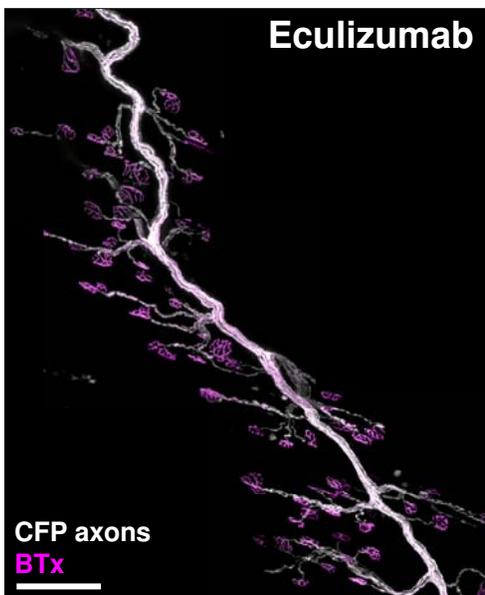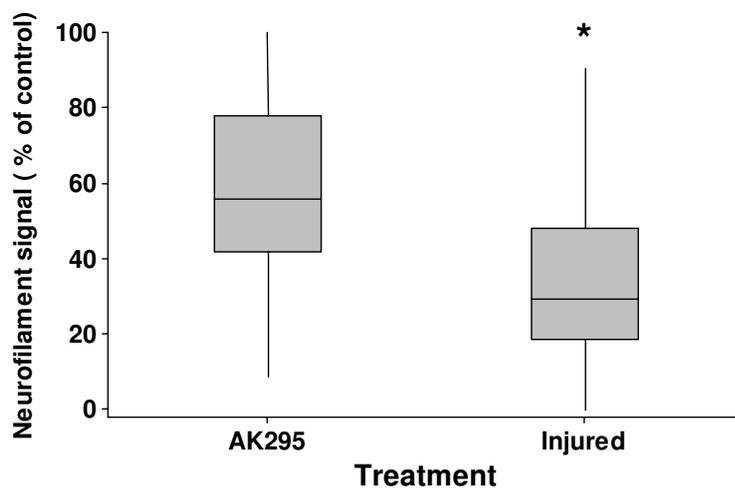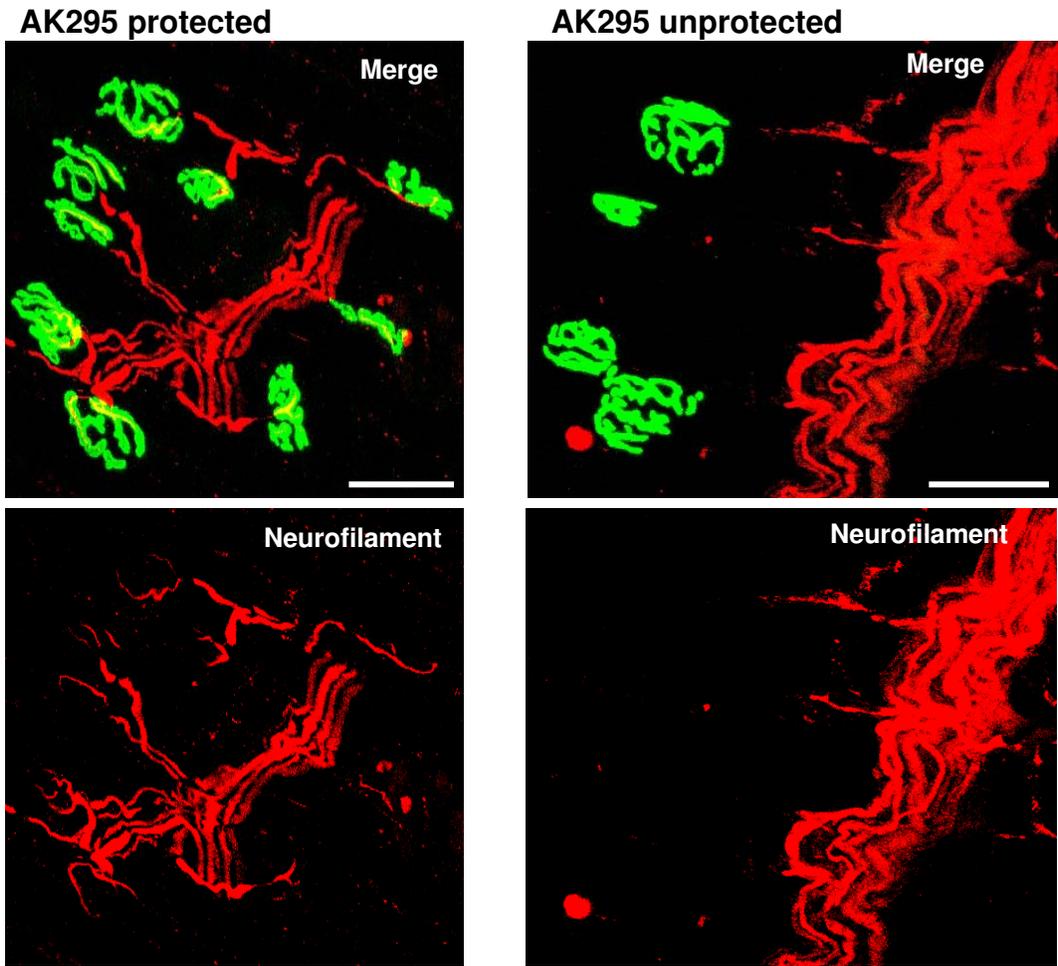
Figure 6

A Nav1.6

B Ankyrin G

C Caspr

D

Figure 7

A

B

C

Figure 8

A

% immunostained NoR

Nav1.6　AnkG　Caspr　moesin　NrCam

□ control
▨ injured

B

% immunostained NoR

Nav1.6　AnkG　Caspr　moesin　NrCam

□ injured
▨ AK295

C

| | Control | Injured | Injured and AK295 protected |
			example A　example B
Nav1.6			
Ankyrin G			
Caspr			
moesin			
NrCAM			

D

Peak amplitude (mV)　Time (mins)　**Treated**

Peak amplitude (mV)　Time (mins)　**AK295**

E

% of starting peak value

Injured　AK295
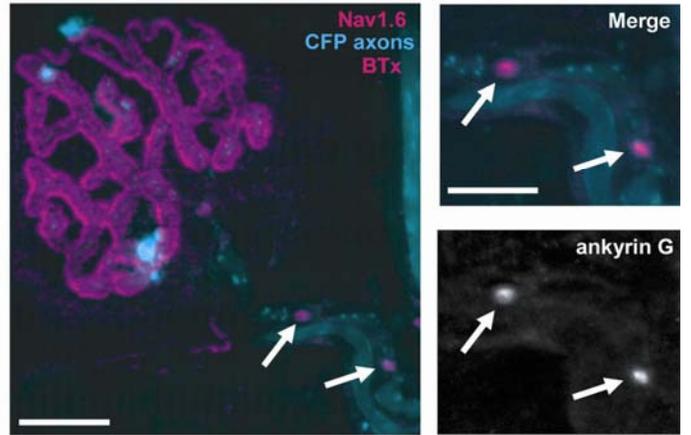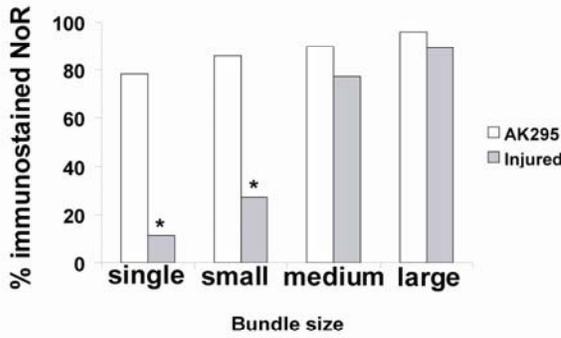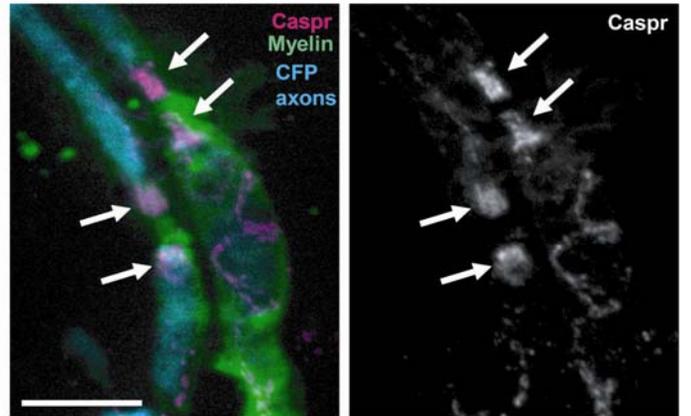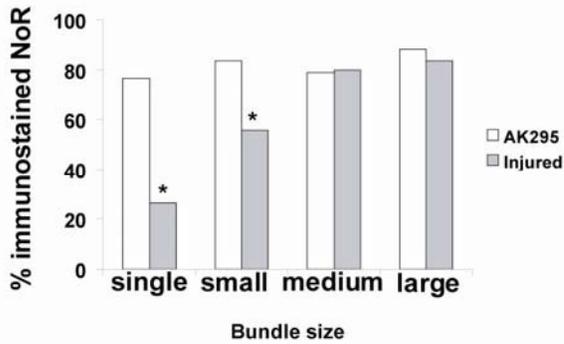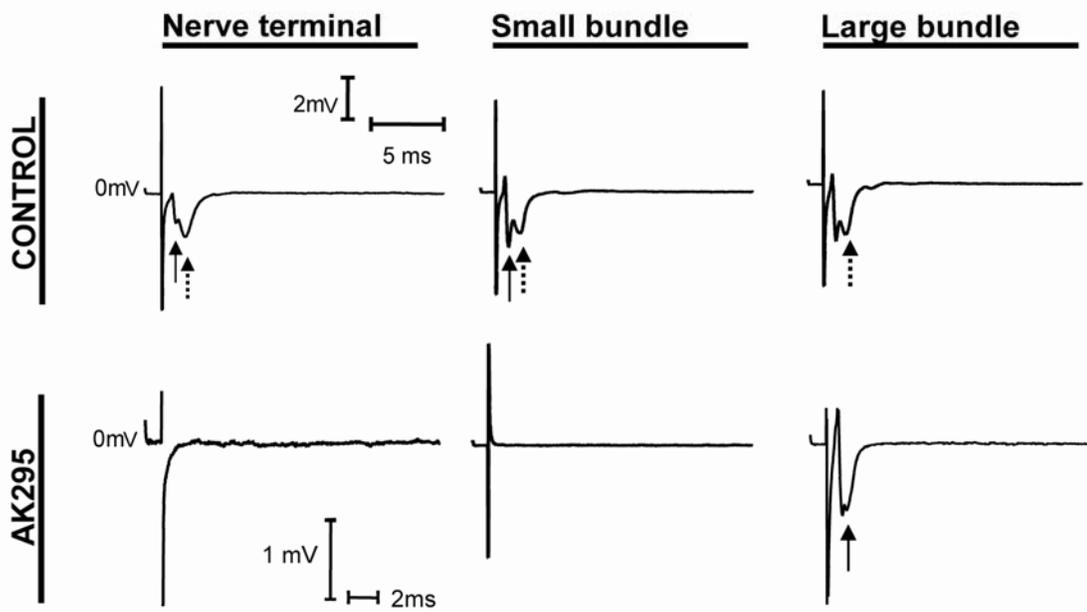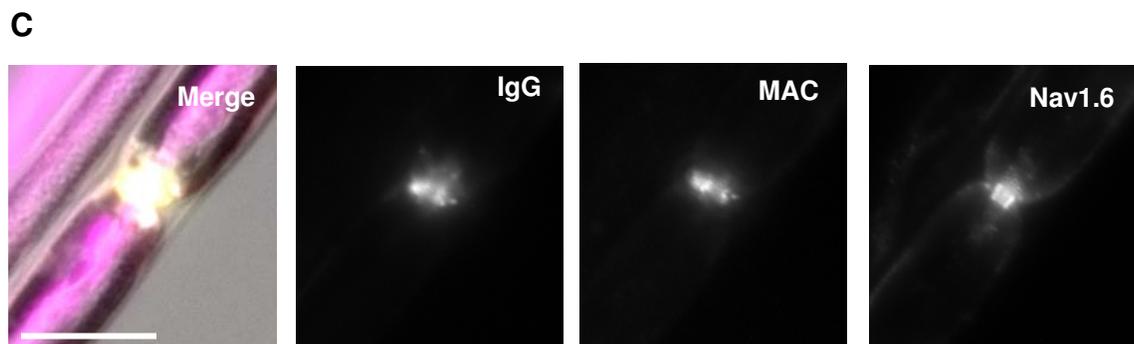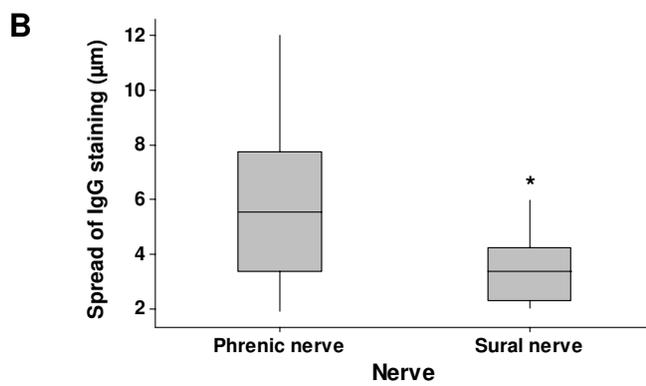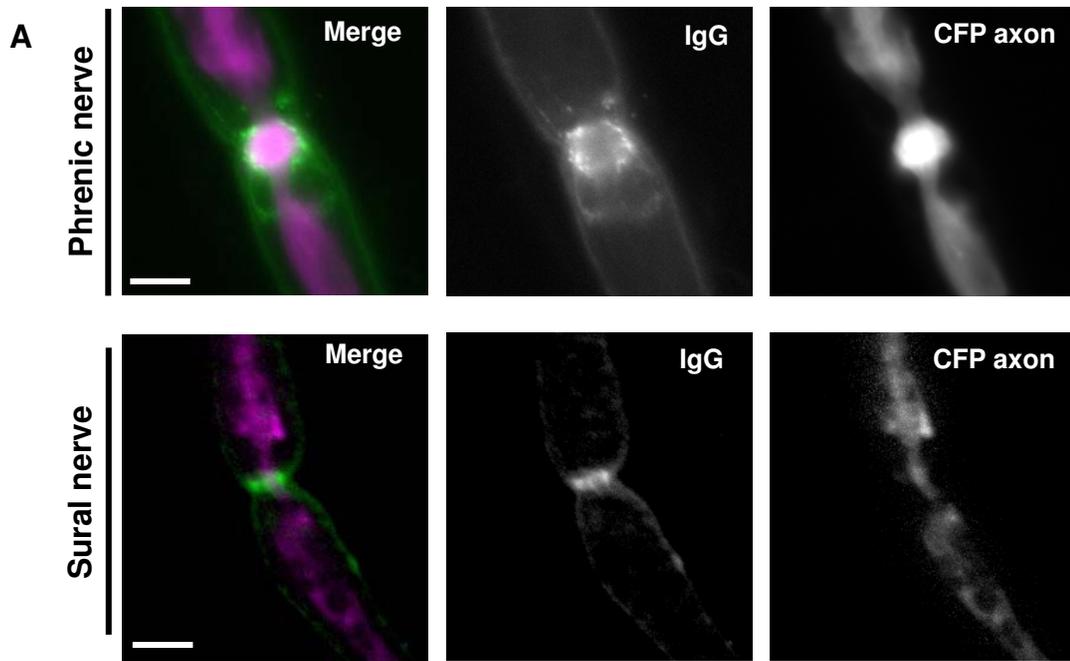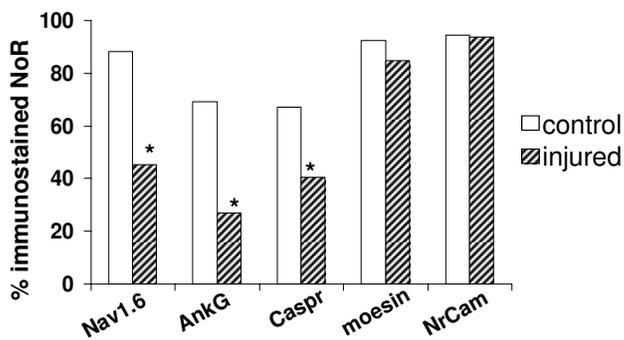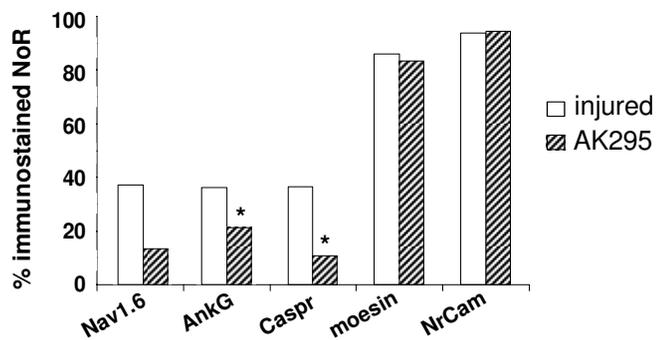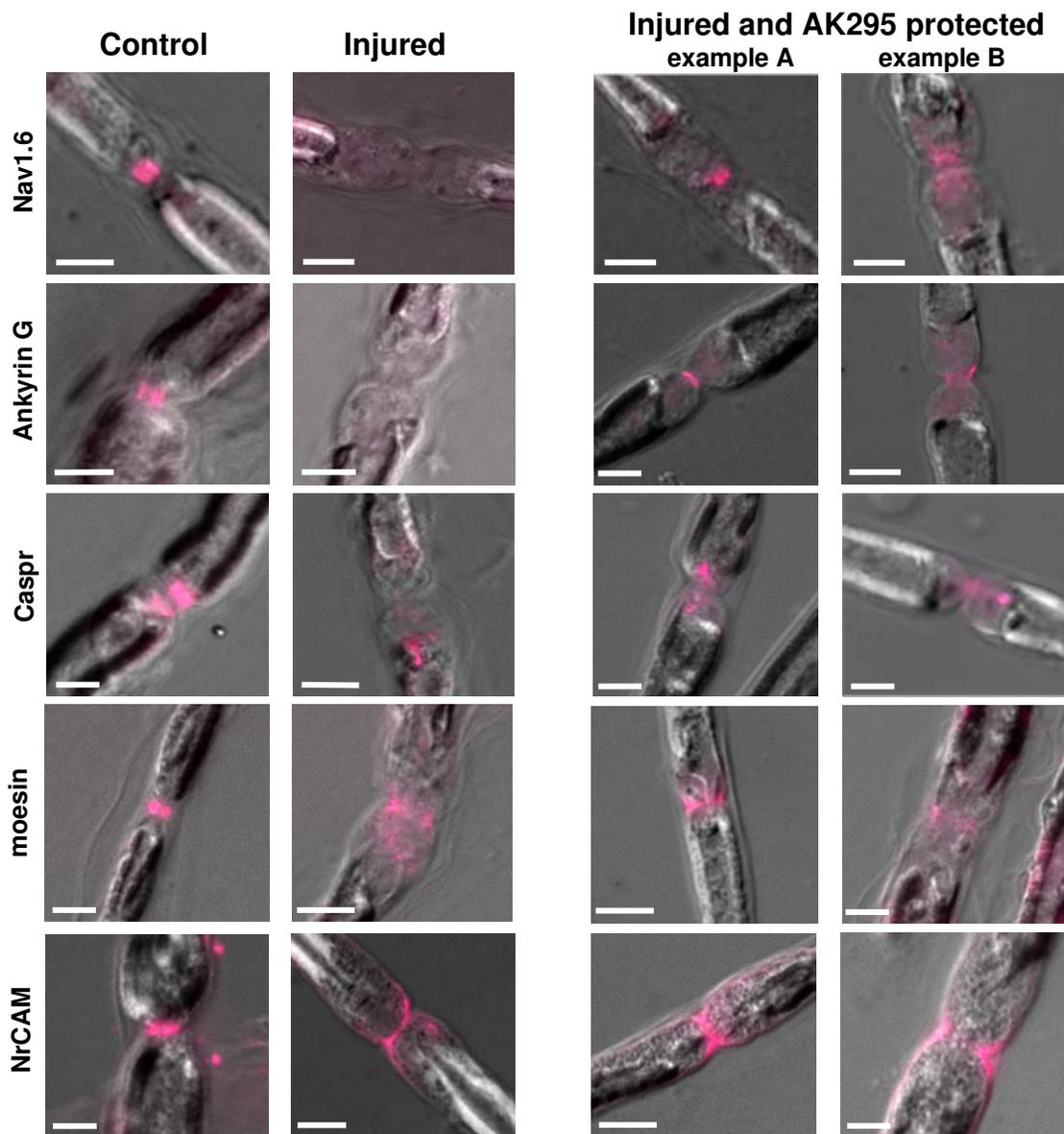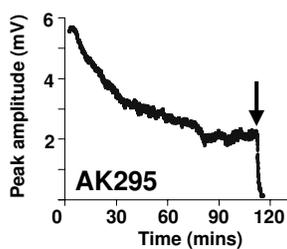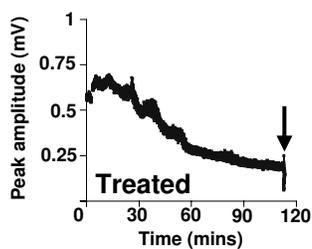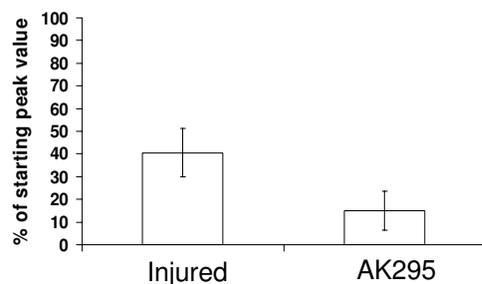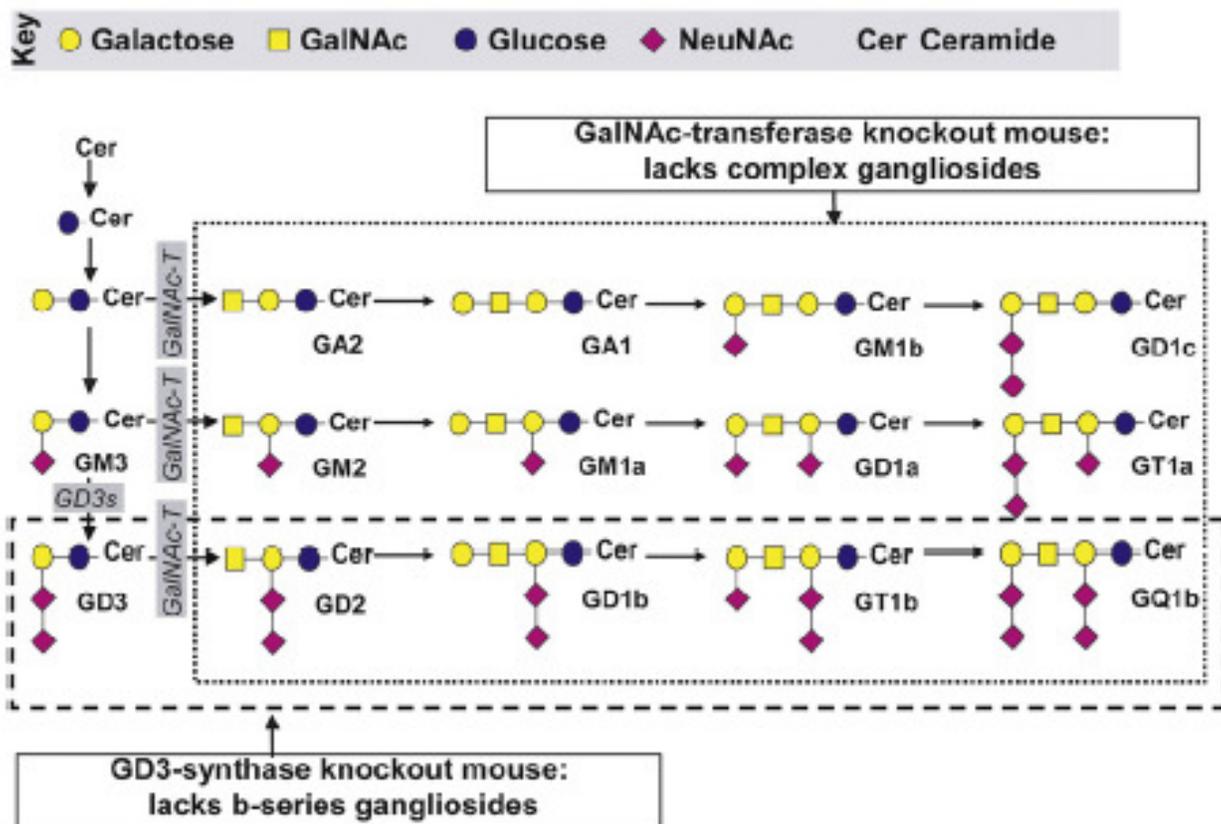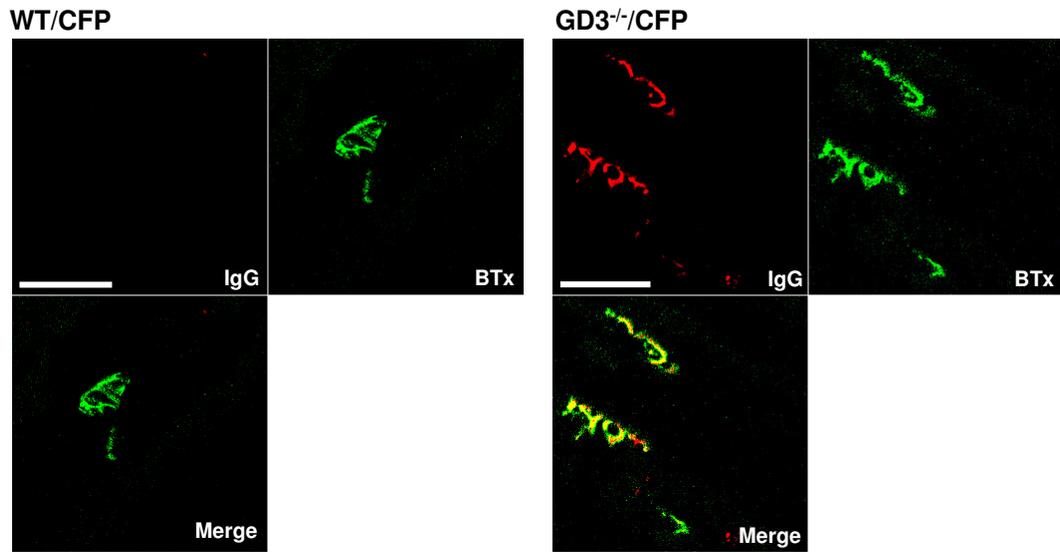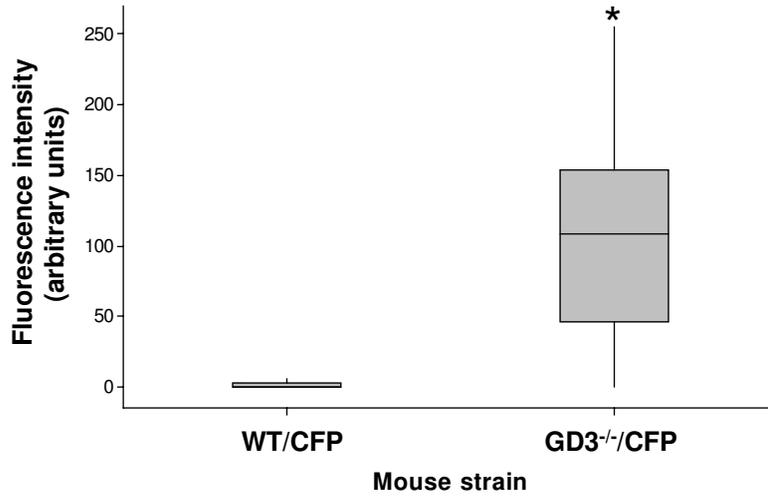
Figure S1

Figure S2

Figure S3
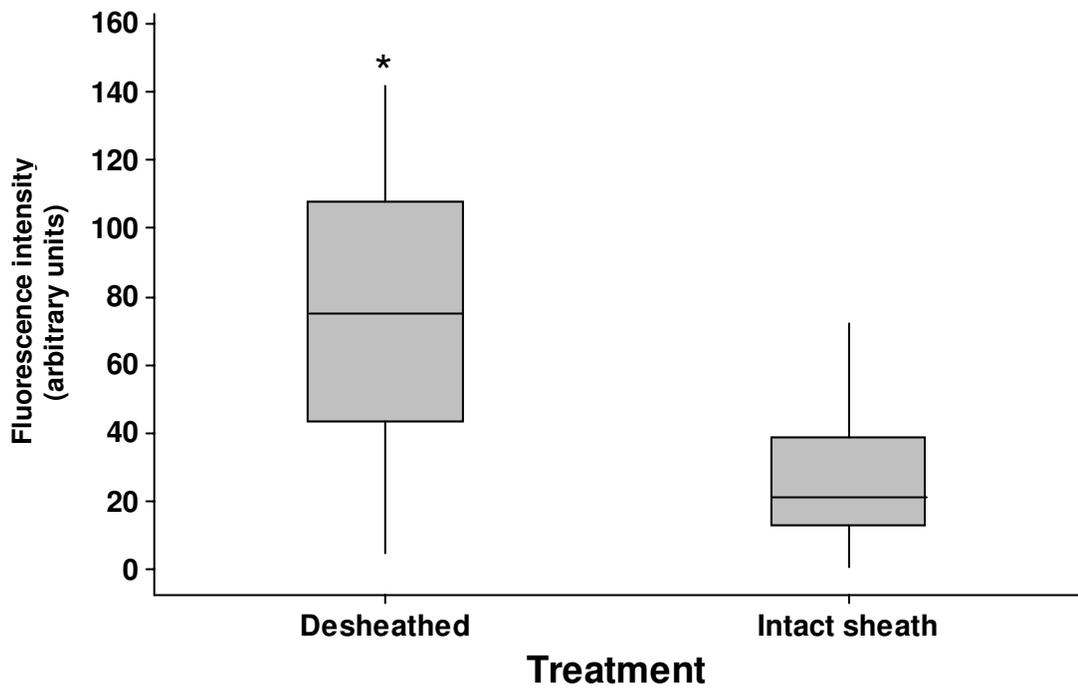
Figure S4
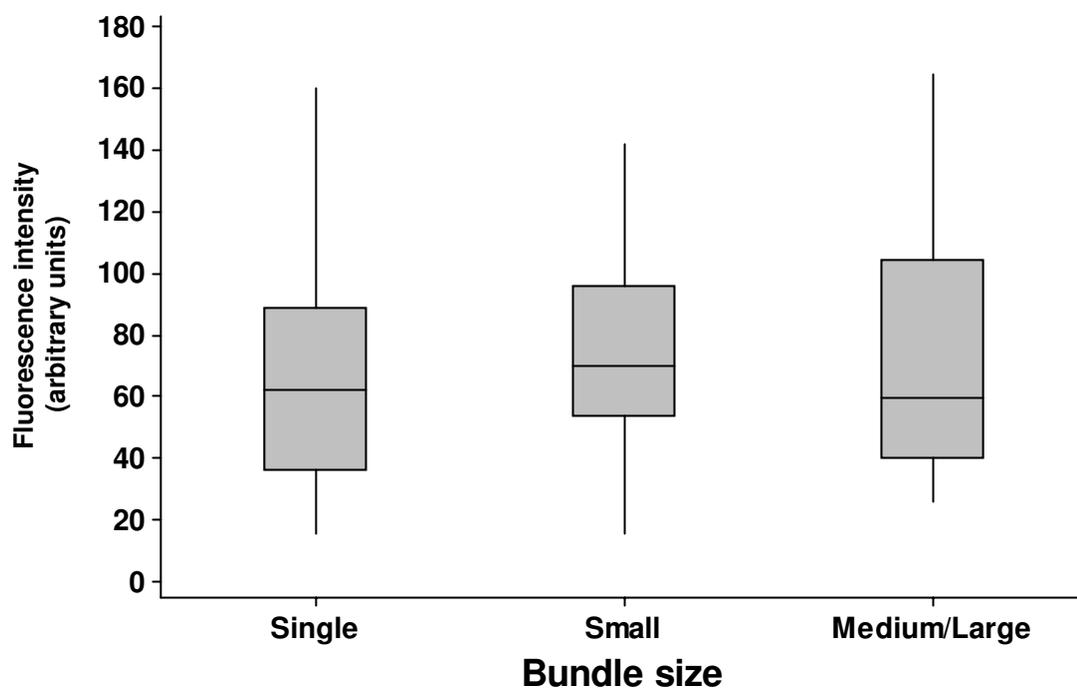
Figure S5
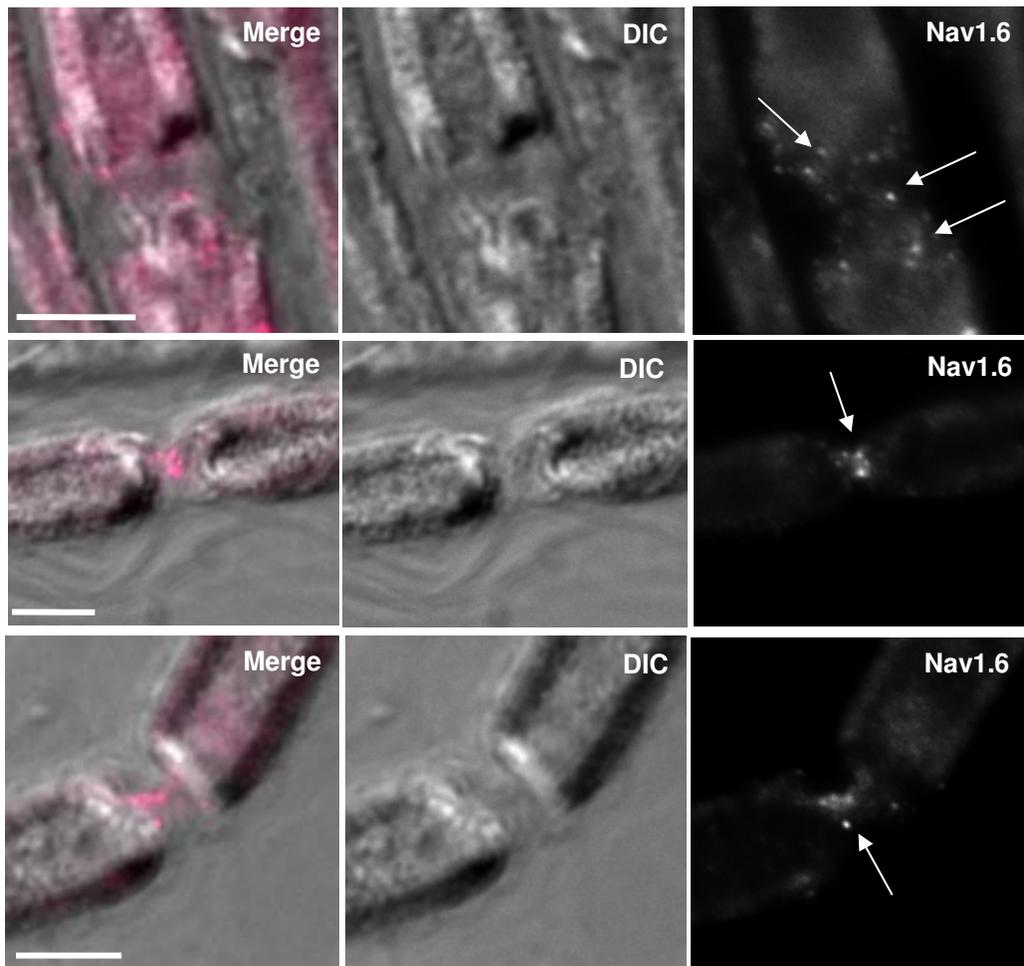
Figure S6
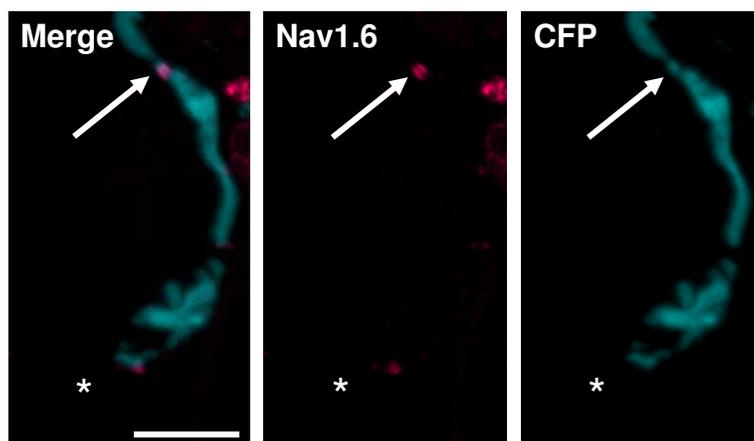
Figure S7

A
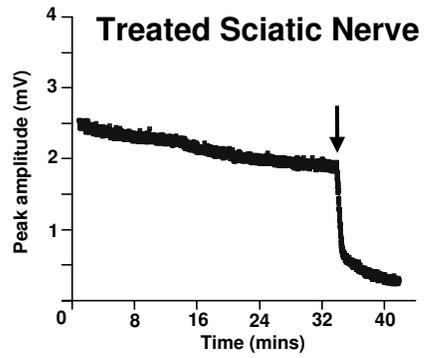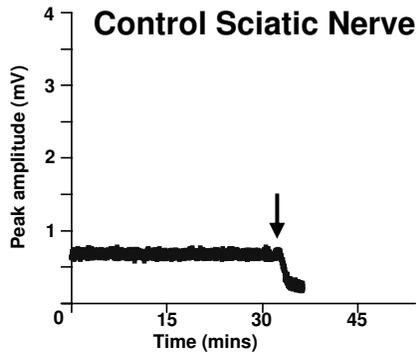
B
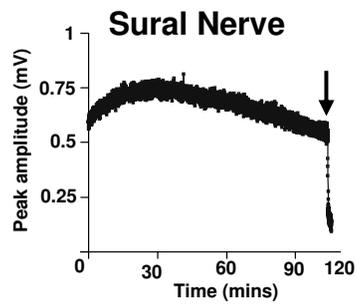
Figure S8
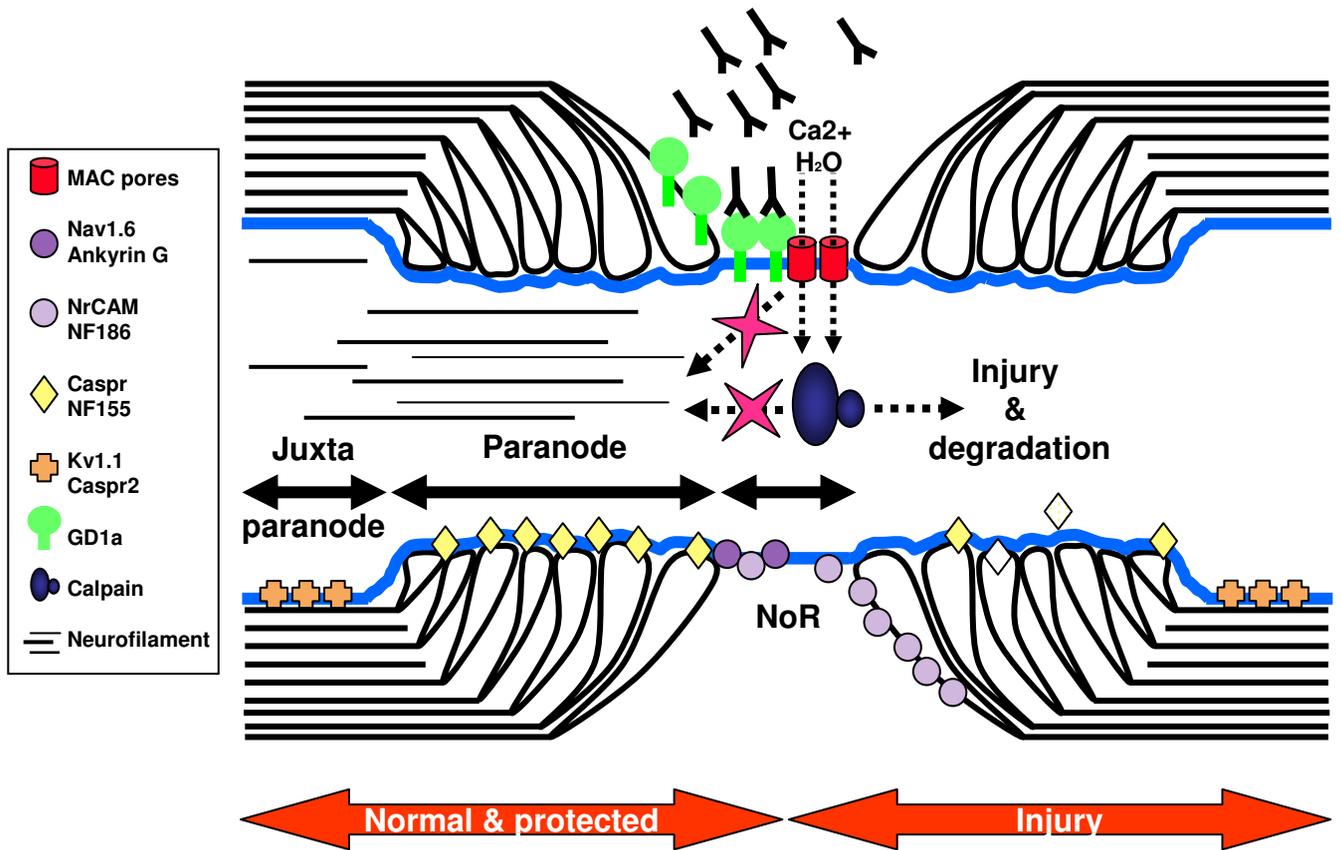
Table 1

Antigen	Host	Isotype	Dilution	Source
Ankyrin G	Mouse	IgG1	1:100	Zymed Labs San Francisco, CA
Caspr	Rabbit	IgG	1:1000	E. Peles, Israel
Dystrophin	Mouse	IgG1	1:200	Sigma Missouri, USA
FluoroMyelin green	-	-	1:400	Molecular Probes Paisley, UK
Kv1.1	Rabbit	IgG	1:200	Alomone Labs Israel
Human MAC (C5b-9)	Mouse	IgG2a	1:50	Dako Glostrup, Denmark
Moesin	Mouse	IgG1	1:100	BIOMOL Int Europe
Nav1.6	Rabbit	IgG	1:100	Sigma Missouri, USA
pan Nav	Mouse	IgG1	1:100	Sigma Missouri, USA
pan Neurofascin	Rabbit	IgG	1:1000	P. Brophy, Edinburgh, UK
Neurofilament	Rabbit	IgG	1:200	Chemicon Int Temecula, CA
NrCAM*	Mouse	IgG1	1:100	Abcam Cambridge, UK